Complete vectorlike fourth family and new $U(1)'$ for muon anomalies

Junichiro Kawamura,[1,2,*] Stuart Raby,[1,†] and Andreas Trautner[3,‡]

[1]*Department of Physics, Ohio State University, Columbus, Ohio 43210, USA*
[2]*Department of Physics, Keio University, Yokohama 223-8522, Japan*
[3]*Max-Planck-Institut für Kernphysik, Saupfercheckweg 1, 69117 Heidelberg, Germany*

(Received 11 July 2019; published 18 September 2019)

We consider the Standard Model (SM) with the addition of a $U(1)'$ gauge symmetry and a complete fourth family of quarks and leptons which are vectorlike with respect to the full $SU(3)_C \times SU(2)_L \times U(1)_Y \times U(1)'$ gauge symmetry. The model provides a unified explanation of experimental anomalies in $(g-2)_\mu$ as well as $b \to s\ell^+\ell^-$ decays. We find good fits to the deviations from the SM, while at the same time fitting all other SM observables. The model includes a new Z' gauge boson, a $U(1)'$-breaking scalar, and vectorlike leptons all with mass of order a few hundred giga-electron-volts. It is consistent with all currently released high energy experimental data; however, it appears imminently testable with well-designed future searches. Also, precision flavor experiments, especially more accurate direct determinations of Cabibbo-Kobayashi-Maskawa matrix elements, would allow probing the best fit points.

DOI: 10.1103/PhysRevD.100.055030

I. INTRODUCTION

The Standard Model (SM) is very successful, explaining most experimental results. However, there are experimental discrepancies with some SM predictions. One is the anomalous magnetic moment of the muon, $(g-2)_\mu$. The current experimental measurement [1,2] shows the discrepancy,

$$\Delta a_\mu \coloneqq a_\mu^{\rm exp} - a_\mu^{\rm SM} = 268(63)(43) \times 10^{-11}. \qquad (1.1)$$

Other discrepancies are reported in observables related to $b \to s\ell^+\ell^-$ processes. The observables testing lepton flavor nonuniversality, R_K and R_{K*}, deviate from the SM prediction [3,4], even though the most recent data are consistent with the SM at 2.5σ [5] or have large error bars [6]. There are also deviations from the SM predictions for semileptonic branching ratios [7–10] and angular distributions [11–17].

It is interesting that all the observables for $b \to s\ell^+\ell^-$ can be explained by new physics (NP) contributions to the effective Hamiltonian [18,19],

$$\mathcal{H}_{\rm eff}^{\ell} = -\frac{4G_F}{\sqrt{2}}\frac{\alpha_e}{4\pi} V_{tb}V_{ts}^* \sum_{a=9,10} (C_a^\ell \mathcal{O}_a^\ell + C_a'^\ell \mathcal{O}_a'^\ell), \qquad (1.2)$$

where $\ell = e, \mu, \tau$ and the operators are defined as[1]

$$\mathcal{O}_9^\ell \coloneqq [\bar{s}\gamma^\mu P_L b][\bar{\ell}\gamma_\mu \ell], \quad \mathcal{O}_{10}^\ell \coloneqq [\bar{s}\gamma^\mu P_L b][\bar{\ell}\gamma_\mu\gamma_5 \ell], \qquad (1.3)$$

$$\mathcal{O}_9'^\ell \coloneqq [\bar{s}\gamma^\mu P_R b][\bar{\ell}\gamma_\mu \ell], \quad \mathcal{O}_{10}'^\ell \coloneqq [\bar{s}\gamma^\mu P_R b][\bar{\ell}\gamma_\mu\gamma_5 \ell]. \qquad (1.4)$$

The analyses before Moriond 2019 [21–29] and after Moriond 2019 [30–37] show that several patterns of NP contributions explain the discrepancies significantly better than the SM. In all cases, there should be a sizable negative contribution to C_9^μ.

The muon anomalous magnetic moment Δa_μ can be explained by introducing vectorlike (VL) leptons which exclusively couple to muons [38–41]. A way to address the $b \to s\ell^+\ell^-$ anomalies is to introduce a Z' gauge boson which couples to muons and down-type quarks. For instance, $U(1)_{\mu\text{-}\tau}$ gauge symmetry and VL quarks [with $U(1)_{\mu\text{-}\tau}$ charge] are introduced to control the flavor dependent couplings of the Z' boson [42,43] [see Ref. [44] for a more general discussion of $U(1)'$ gauge symmetry]. It is shown in Refs. [45–49] that both of the Δa_μ and $b \to s\ell^+\ell^-$ anomalies are successfully explained in models with VL leptons, VL quarks, and a Z' boson.

Box-diagram contributions involving new fermions and scalars can also account for the $b \to s\ell^+\ell^-$ anomalies [50–53]. They may even include particle candidates for dark matter [54–58]. These extensions, however, typically

*kawamura.14@osu.edu
†raby.1@osu.edu
‡trautner@mpi-hd.mpg.de

Published by the American Physical Society under the terms of the Creative Commons Attribution 4.0 International license. Further distribution of this work must maintain attribution to the author(s) and the published article's title, journal citation, and DOI. Funded by SCOAP³.

[1]Effective operators for fitting the process $b \to se^+e^-$ were first given in Ref. [20].

induce deviations from the SM predictions for lepton flavor violating (LFV) decays, Higgs decays, and B_s-$\bar{B}_s$ mixing.

In this paper, we propose a model with a complete fourth family of fermions which are VL under both the SM and a U(1)′ gauge symmetry. Similar models with chiral U(1)′ gauge symmetry are considered in Refs. [42,48]. In these models, the SM families typically have sizable couplings to the Z' gauge boson in the gauge basis. A VL U(1)′ where a new singlet scalar [59] or the singlet VL neutrino are dark matter candidates has been studied [60]. However, the parameter space there is very restricted, so Δa_μ was not addressed. In our present model, all Z' couplings to the SM fermions are controlled by the mixing of the SM families with the VL family. We find that a certain pattern of mixings can simultaneously address both Δa_μ and the $b \to s\ell^+\ell^-$ anomalies.

We analyze this model involving all three SM families. This allows us to explicitly discuss both the Cabibbo-Kobayashi-Maskawa (CKM) matrix and exotic particle production from quarks and gluons at the LHC. We find points in the parameter space which explain the muon anomalies and all other observables by using a χ^2 fit. The purpose of this paper is to demonstrate the existence of points which are consistent with the anomalies, as well as all other SM observables, and study the expected phenomenology at these points. A more detailed analysis of the expected phenomenology in a wider parameter space is delegated to future work.

The rest of this paper is organized as follows. The model is introduced in Sec. II; then, we discuss the most relevant observables for the muon anomalies in Sec. III. In Sec. IV, we show the best fit points of our χ^2 analysis and study their phenomenology. Section V is devoted to our conclusions. Values of the input parameters and all observables calculated in this analysis are listed in the Appendix.

II. MODEL

A. Matter content and masses

In this paper, we study a model with a complete VL fourth family and U(1)′ gauge symmetry. The quantum numbers of all fields are listed in Tables I and II. The SM $\mathrm{SU(2)_L}$ doublets are defined as $q_{Li} = (u_{Li}, d_{Li})$, $l_{Li} = (\nu_{Li}, e_{Li})$, and $H = (H_0, H_-)$. The new doublets are $Q_L = (U'_L, D'_L)$, $L_L = (N'_L, E'_L)$, $\bar{Q}_R = (-\bar{D}'_R, \bar{U}'_R)$, and $\bar{L}_R = (-\bar{E}'_R, \bar{N}'_R)$. The model is trivially anomaly free since the U(1)′ charge assignment is completely vectorlike.

TABLE I. Quantum numbers of SM particles. Here, $i = 1, 2, 3$ runs over the three SM families. Electromagnetic charges are given by $Q_f = T^3_f + Y_f/2$.

	q_{Li}	$\bar{u}_{Ri}$	$\bar{d}_{Ri}$	l_{Li}	$\bar{e}_{Ri}$	$\bar{\nu}_{Ri}$	H
$\mathrm{SU(3)_C}$	**3**	$\bar{\mathbf{3}}$	$\bar{\mathbf{3}}$	**1**	**1**	**1**	**1**
$\mathrm{SU(2)_L}$	**2**	**1**	**1**	**2**	**1**	**1**	**2**
$\mathrm{U(1)_Y}$	1/3	−4/3	2/3	−1	2	0	−1
U(1)′	0	0	0	0	0	0	0

In the gauge basis, there are no couplings between the SM families and the Z' boson. These are induced in the mass basis by mixing effects. The Yukawa couplings in the gauge basis are given by

$$\mathcal{L}_{\mathrm{Yukawa}} = \mathcal{L}_{\mathrm{SM}} + \mathcal{L}_{\mathrm{H}} + \mathcal{L}_\phi + \mathcal{L}_\Phi + \mathrm{H.c.}, \quad (2.1)$$

where

$$\mathcal{L}_{\mathrm{SM}} \coloneqq \bar{u}_{Ri} y^u_{ij} q_{Lj} \tilde{H} + \bar{d}_{Ri} y^d_{ij} q_{Lj} H + \bar{e}_{Ri} y^e_{ij} l_{Lj} H + \bar{\nu}_{Ri} y^n_{ij} l_{Lj} \tilde{H}, \quad (2.2)$$

$$\mathcal{L}_{\mathrm{H}} \coloneqq \lambda_u \bar{U}_R Q_L \tilde{H} + \lambda_d \bar{D}_R Q_L H + \lambda_e \bar{E}_R L_L H + \lambda_n \bar{N}_R L_L \tilde{H} + \lambda'_u \bar{Q}_R H U_L - \lambda'_d \bar{Q}_R \tilde{H} D_L - \lambda'_e \bar{L}_R \tilde{H} E_L + \lambda'_n \bar{L}_R H N_L, \quad (2.3)$$

$$\mathcal{L}_\phi \coloneqq \phi(\lambda^Q_V \bar{Q}_R Q_L - \lambda^U_V \bar{U}_R U_L - \lambda^D_V \bar{D}_R D_L + \lambda^L_V \bar{L}_R L_L - \lambda^E_V \bar{E}_R E_L - \lambda^N_V \bar{N}_R N_L), \quad (2.4)$$

$$\mathcal{L}_\Phi \coloneqq \Phi(\lambda^Q_i \bar{Q}_R q_{Li} + \lambda^L_i \bar{L}_R l_{Li}) - \Phi^*(\lambda^U_i \bar{u}_{Ri} U_L + \lambda^D_i \bar{d}_{Ri} D_L + \lambda^E_i \bar{e}_{Ri} E_L + \lambda^N_i \bar{\nu}_{Ri} N_L). \quad (2.5)$$

Here, we have used $\tilde{H} \coloneqq i\sigma_2 H^* = (H^*_-, -H^*_0)$ and $i, j = 1, 2, 3$ run over the three SM generations.

The scalar fields acquire vacuum expectation values (VEVs) given by $v_H \coloneqq \langle H \rangle$, $v_\phi \coloneqq \langle \phi \rangle$, and $v_\Phi \coloneqq \langle \Phi \rangle$. The charged lepton mass matrix then is given by

$$\bar{e}^A_R \mathcal{M}^e_{AB} e^B_L = \begin{pmatrix} \bar{e}_{Ri} & \bar{E}_R & \bar{E}'_R \end{pmatrix} \begin{pmatrix} y^e_{ij} v_H & 0_i & \lambda^E_i v_\Phi \\ 0_j & \lambda_e v_H & \lambda^E_V v_\phi \\ \lambda^L_j v_\Phi & \lambda^L_V v_\phi & \lambda'_e v_H \end{pmatrix} \times \begin{pmatrix} e_{Lj} \\ E'_L \\ E_L \end{pmatrix}, \quad (2.6)$$

where $A, B = 1, \ldots, 5$. We define the mass basis via

$$[\hat{e}_L]_A \coloneqq [(U^e_L)^\dagger]_{AB} [e_L]_B, \qquad [\hat{e}_R]_A \coloneqq [(U^e_R)^\dagger]_{AB} [e_R]_B, \quad (2.7)$$

with unitary matrices that satisfy

$$(U^e_R)^\dagger \mathcal{M}^e U^e_L = \mathrm{diag}(m_e, m_\mu, m_\tau, m_{E_1}, m_{E_2}). \quad (2.8)$$

Here, m_{E_1} and m_{E_2} are masses for the extra charged leptons, which are predominantly the VL leptons of the gauge basis. The mass matrices for the up and down quarks are obtained

TABLE II. Quantum numbers of the new VL fourth family and new scalar fields.

	Q_L	$\bar{U}_R$	$\bar{D}_R$	L_L	$\bar{E}_R$	$\bar{N}_R$	$\bar{Q}_R$	U_L	D_L	$\bar{L}_R$	E_L	N_L	ϕ	Φ
$\mathrm{SU(3)_C}$	**3**	$\bar{\mathbf{3}}$	$\bar{\mathbf{3}}$	**1**	**1**	**1**	$\bar{\mathbf{3}}$	**3**	**3**	**1**	**1**	**1**	**1**	**1**
$\mathrm{SU(2)_L}$	**2**	**1**	**1**	**2**	**1**	**1**	**2**	**1**	**1**	**2**	**1**	**1**	**1**	**1**
$\mathrm{U(1)_Y}$	1/3	−4/3	2/3	−1	2	0	−1/3	4/3	−2/3	1	−2	0	0	0
$\mathrm{U(1)'}$	−1	1	1	−1	1	1	1	−1	−1	1	−1	−1	0	−1

from $\mathcal{M}^e$ by formally replacing $e \to u$, $E \to U$, or $e \to d$, $E \to D$, respectively.

As a consequence of the $\mathrm{U(1)'}$ charges, only the three standard generations of right-handed (RH) neutrinos have Majorana masses,

$$\mathcal{L}_{\mathrm{Maj}} = -\frac{1}{2}\bar{\nu}_{R_i} M^{ij}_{\mathrm{Maj}} \nu^c_{R_j}. \tag{2.9}$$

The neutrino Dirac mass matrix is obtained from $\mathcal{M}^e$ by formally replacing $e \to n$ and $E \to N$. The Majorana masses are assumed to be $\mathcal{O}(10^{14})$ GeV, thereby explaining the tiny observed neutrino masses via a standard type I seesaw mechanism. As usual, three generations of left-handed (LH) neutrinos have tiny masses of $\mathcal{O}(v_H^2/M_{\mathrm{Maj}})$, while three generations of RH neutrinos have huge masses $\mathcal{O}(M_{\mathrm{Maj}})$. Unlike in the standard type I seesaw case, there are four more degrees of freedom here, which form two Dirac fermions with masses of $\mathcal{O}(\mathrm{TeV})$. The mixing of those with the other neutrinos is negligible as it is suppressed by the Majorana mass terms.

The neutral scalar fields are expanded as

$$H_0 = v_H + \frac{1}{\sqrt{2}}(h + i a_h), \qquad \Phi = v_\Phi + \frac{1}{\sqrt{2}}(\chi + i a_\chi),$$
$$\phi = v_\phi + \sigma. \tag{2.10}$$

The CP-odd degrees of freedom, namely a_h and a_χ, get eaten by the gauge fields, and only the real components h and χ are physical. We assume that ϕ is a real scalar field.

We parametrize the masses for χ and σ as

$$m_\chi^2 = \lambda_\chi v_\Phi^2 \quad \text{and} \quad m_\sigma^2 = \lambda_\sigma v_\phi^2. \tag{2.11}$$

Here, we have introduced the *effective* quartic couplings λ_χ and λ_σ. The scalar χ should not be much heavier than the Z' boson, as long as the effective quartic coupling stays perturbative and the new gauge coupling g' is not tiny. Importantly, the couplings of χ are responsible for the mass mixing of SM particles with the VL families. Consequently, to the extent that this mixing is necessary to fit the muon anomalies, χ contributes significantly in our fits. On the other hand, v_ϕ could be very large compared with v_Φ as long as the Yukawa couplings to ϕ, e.g., λ_V^L and λ_V^E, are small enough to prevent the VL fermions from decoupling much above the tera-electron-volt scale. The scalar σ can thus be heavy and therefore irrelevant for current observables. Indeed, contributions from σ will be negligible at the best fit points shown below.

B. Yukawa and gauge couplings

The real scalar fields couple to the charged leptons as

$$-\mathcal{L}_{\mathrm{Yukawa}} = \frac{1}{\sqrt{2}} h \bar{e}_R Y_e^h e_L + \frac{1}{\sqrt{2}} \chi \bar{e}_R Y_e^\chi e_L + \mathrm{H.c.}, \tag{2.12}$$

where, in the gauge basis,

$$Y_e^h = \begin{pmatrix} y^e_{ij} & 0_i & 0_i \\ 0_j & \lambda_e & 0 \\ 0_j & 0 & \lambda'_e \end{pmatrix}, \qquad Y_e^\chi = \begin{pmatrix} 0_{ij} & 0_i & \lambda^E_i \\ 0_j & 0 & 0 \\ \lambda^L_j & 0 & 0 \end{pmatrix}, \tag{2.13}$$

and completely analogous coupling structure for the quarks. The Yukawa coupling matrices in the mass basis are given by

$$\hat{Y}_e^S = (U_R^e)^\dagger Y_e^S U_L^e, \quad \text{where } S = h, \chi. \tag{2.14}$$

Combining LH and RH fields *à la* $f^A \coloneqq (f_L^A, f_R^A)$, the W boson couplings are given by

$$\mathcal{L}_W = \frac{g}{\sqrt{2}} W_\mu^+ [\bar{u}\gamma^\mu (P_{\bar{5}} P_L + P_5 P_R) d$$
$$+ \bar{\nu}\gamma^\mu (P_{\bar{5}} P_L + P_5 P_R) e] + \mathrm{H.c.}, \tag{2.15}$$

where we have used the flavor space projectors

$$P_5 \coloneqq \mathrm{diag}(0,0,0,0,1), \quad \text{and} \quad P_{\bar{5}} \coloneqq \mathbb{1}_5 - P_5. \tag{2.16}$$

The couplings in the mass basis are[2]

$$\hat{g}^W_{q_L} = \frac{g}{\sqrt{2}} (U_L^u)^\dagger P_{\bar{5}} U_L^d, \quad \hat{g}^W_{q_R} = \frac{g}{\sqrt{2}} (U_R^u)^\dagger P_5 U_R^d, \tag{2.17}$$

$$\hat{g}^W_{\ell_L} = \frac{g}{\sqrt{2}} (U_L^n)^\dagger P_{\bar{5}} U_L^e, \quad \hat{g}^W_{\ell_R} = \frac{g}{\sqrt{2}} (U_R^n)^\dagger P_5 U_R^e. \tag{2.18}$$

[2]Note that here and in the following we neglect effects of $\mathcal{O}(v_H^2/M_{\mathrm{Maj}})$, implying that we can treat the left- and right-handed neutrino rotations separately.

Note that there are also right-handed charged current interactions, unlike in the SM.

The extended CKM matrix is a 5×5 matrix,

$$\hat{V}_{\mathrm{CKM}} = (U_L^u)^\dagger P_{\bar{5}} U_L^d. \tag{2.19}$$

The 3×3 CKM matrix for the three SM families is not unitary because of the mixing with the VL family. We remark that also the 5×5 matrix $\hat{V}_{\mathrm{CKM}}$ is not unitary.

The Z boson couplings are given by[3]

$$\mathcal{L}_Z = \frac{g}{c_W} Z_\mu \sum_{f=u,d,e,n} \bar{f} \gamma^\mu [(T_3^f P_{\bar{5}} - Q_f s_W^2) P_L + (T_3^f P_5 - Q_f s_W^2) P_R] f. \tag{2.20}$$

The couplings for a fermion $f = u, d, e, n$ in the mass basis are given by

$$\hat{g}_{f_L}^Z = \frac{g}{c_W} [(U_L^f)^\dagger P_{\bar{5}} U_L^f - Q_f s_W^2],$$
$$\hat{g}_{f_R}^Z = \frac{g}{c_W} [(U_R^f)^\dagger P_5 U_R^f - Q_f s_W^2]. \tag{2.21}$$

Finally, the couplings to the Z' boson are given by

$$\mathcal{L}_{Z'} = g' Z'_\mu \sum_{f=u,d,e,\nu} \bar{f} \gamma^\mu (Q'_{f_L} P_L + Q'_{f_R} P_R) f = Z'_\mu \sum_{f=u,d,e,n} \bar{\hat{f}} \gamma^\mu (\hat{g}_{f_L}^{Z'} P_L + \hat{g}_{f_R}^{Z'} P_R) \hat{f}, \tag{2.22}$$

where the fermions in the mass basis are denoted by $\hat{f}$ and the charge matrices are

$$Q'_{f_L} = Q'_{f_R} = \mathrm{diag}(0, 0, 0, -1, -1). \tag{2.23}$$

In the mass basis,

$$\hat{g}_{f_L}^{Z'} = g' (U_L^f)^\dagger Q'_{f_L} U_L^f \quad \text{and} \quad \hat{g}_{f_R}^{Z'} = g' (U_R^f)^\dagger Q'_{f_R} U_R^f, \tag{2.24}$$

implying that all couplings between Z' and the SM fermions are controlled by the mixing matrices.

Altogether, we find that the model has nonunitary CKM mixing and tree-level flavor changing neutral currents mediated by Z, Z'; the SM Higgs boson; as well as by the new boson χ. In addition, W bosons also acquire couplings to the right-handed charged currents of SM fermions, which are constrained by measurements such as neutrino-nucleon scattering [61]. All of these effects are in general severely constrained by experiments. However, we find that in our model all those effects are controlled by $\mathcal{O}(m_f^2/M_{\mathrm{VL}}^2)$ coefficients, implying that they are generally suppressed. We prove this analytically in Appendix A. In agreement with this, both the unitarity of the 3×3 CKM and Pontecorvo-Maki-Nakagawa-Sakata (PMNS) matrix as well as the absence of all tree-level flavor violating effects for SM fermions are restored in the limit of a heavy VL family. That is, the model approaches the SM in the decoupling limit.

[3]Here, we abbreviate the (co)sine of the weak mixing angle as $s_W (c_W)$; T_3^f and Q_f are, respectively, the third component of weak isospin and the electromagnetic charge of the fermion f; and five-dimensional identity matrices $\mathbb{1}_5$ in flavor space are implicit where appropriate.

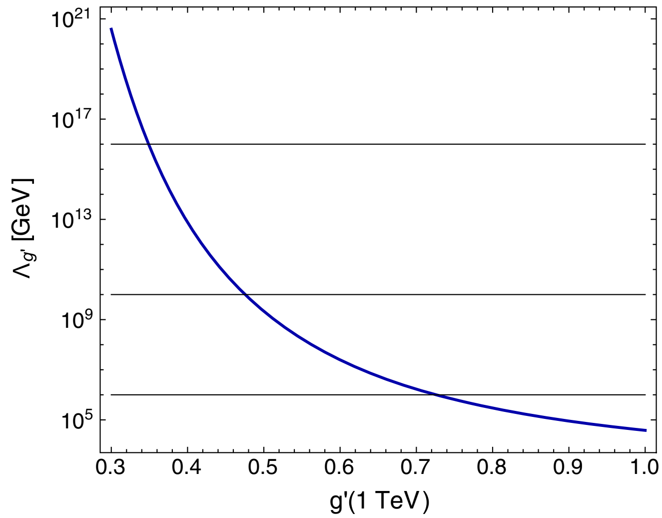

FIG. 1. Scale of the $\mathrm{U}(1)'$ Landau pole as a function of g' at 1 TeV.

C. Renormalization group equation evolution of the $\mathbf{U(1)'}$ gauge coupling

The $\mathrm{U}(1)'$ gauge coupling constant g' should be sufficiently small at the tera-electron-volt scale such that it stays perturbative under renormalization group equation running up to a scale where UV physics, such as a grand unified theory (GUT), emerges. The one-loop beta function for g' is given by

$$\frac{dg'}{d \ln \mu} = \frac{g'^3}{16\pi^2} \frac{65}{3}. \tag{2.25}$$

This gives rise to a scale of the Landau pole for g',

$$\Lambda_{g'} = \mu_{Z'} \exp\left(\frac{24\pi^2}{65 g'(\mu_{Z'})^2}\right), \tag{2.26}$$

where $\mu_{Z'} \sim 1$ TeV is the typical scale of the model. Figure 1 shows the scale of the Landau pole in dependence of $g'(\mu_{Z'})$ at the tera-electron-volt scale. For example, $g'(1\ \mathrm{TeV}) \lesssim 0.35(0.48)$ is required for $\Lambda_{g'} \sim 10^{16}(10^{10})$ GeV. In our numerical analysis, we focus on a situation where the model is correct up to a typical GUT scale of 10^{16} GeV, such that $g'(1\ \mathrm{TeV}) < 0.35$ is required.

III. OBSERVABLES

In this model, Δa_μ is explained by one-loop contributions involving the Z' boson and VL leptons. NP contributions to $C_{9,10}^{(\prime)\mu}$ are provided by tree-level Z' exchange. NP contributions will also affect observables which are currently consistent with the SM such as $\mathrm{Br}(\mu \to e\gamma)$, $\mathrm{Br}(\tau \to \mu\gamma)$, $\mathrm{Br}(\tau \to \mu\mu\mu)$, B_q-$\bar{B}_q$ mixing, etc. The most relevant observables for the muon anomalies will be discussed in the following. An in-depth discussion of these and further observables is postponed to future work.

A. Δa_μ and $\mathrm{U}(1)'$ charge assignment

The dominant Z'-boson contribution to Δa_μ is given by (see e.g., Refs. [40,62])

$$\delta_{Z'} a_\mu \simeq -\frac{m_\mu}{8\pi^2 m_{Z'}^2} \sum_{a=1,2} \mathrm{Re}([\hat{g}^{Z'}_{\hat{e}_L}]_{\mu E_a} [\hat{g}^{Z'}_{\hat{e}_R}]^*_{\mu E_a}) m_{E_a} G_Z(x_a), \tag{3.1}$$

where $x_a \coloneqq m_{E_a}^2/m_{Z'}^2$ and the loop function is given by

$$G_Z(x) \coloneqq \frac{x^3 + 3x - 6x\ln(x) - 4}{2(1-x)^3}. \tag{3.2}$$

The dominant contribution of the scalar χ is given by

$$\delta_\chi a_\mu \simeq -\frac{m_\mu}{32\pi^2 m_\chi^2} \sum_{a=1,2} \mathrm{Re}([\hat{Y}^\chi_e]_{\mu E_a} [\hat{Y}^\chi_e]_{E_a \mu}) m_{E_a} G_S(y_a), \tag{3.3}$$

where $y_a \coloneqq m_{E_a}^2/m_\chi^2$ and the loop function is

$$G_S(x) \coloneqq \frac{x^2 - 4x + 2\ln(x) + 3}{(1-x)^3}. \tag{3.4}$$

There are also new contributions from loops involving the SM bosons and the VL fermions, but these are negligible.

Figure 2 shows typical values of the muon mass m_2 and the Z' contribution to δa_μ. For illustration, $g' = 0.25$, $m_{Z'} = \lambda_2^{L,E} v_\Phi = \lambda_V^{L,E} v_\phi = 500$ GeV, and $y^e_{22} v_H = 0.1$ GeV have been fixed, while all other couplings except λ_e and λ'_e are set to zero. We see that $|\lambda'_e| \gtrsim 0.4$ and $\lambda_e \lesssim 10^{-3}$ are required in order to obtain $\Delta a_\mu \gtrsim 10^{-9}$ and $m_\mu \sim 0.1$ GeV. This illustrates how the muon mass is affected by the mixing and enhanced above $m_\mu \sim 0.1$ GeV for $\lambda_e \gtrsim 10^{-3}$.

We see that the Higgs coupling λ'_e *must* exist in the model to explain Δa_μ. This explains the nonuniversal charge assignment in Table II; the $\mathrm{U}(1)'$ charges of VL fermions need to be opposite for $\mathrm{SU}(2)_\mathrm{L}$ doublets and singlets in order to allow the coupling λ'_e. For this reason, the $\mathrm{U}(1)'$ gauge symmetry is incompatible with SU(5) unification. However, it is still compatible with the Pati-Salam gauge group $\mathrm{SU}(4) \times \mathrm{SU}(2)_\mathrm{L} \times \mathrm{SU}(2)_\mathrm{R}$.

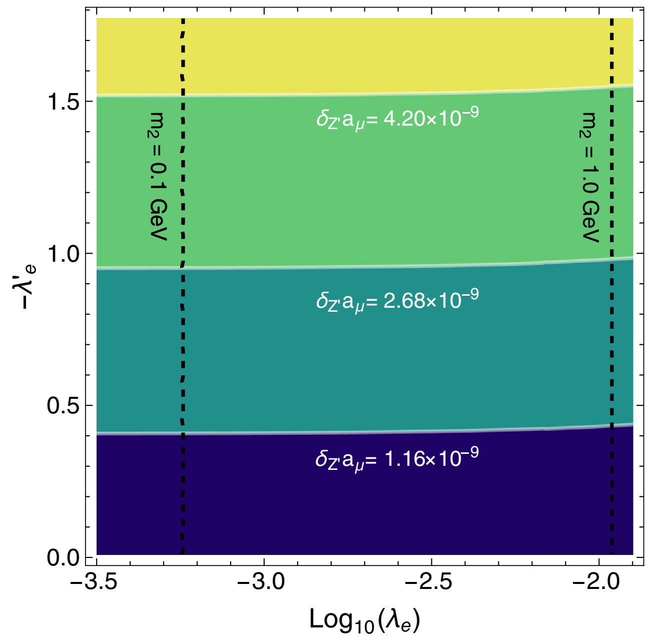

FIG. 2. The muon mass m_2 and $\delta_{Z'} a_\mu$ in dependence of λ_e and λ'_e.

B. $\mathrm{Br}(\ell_i \to \ell_j \gamma)$

The branching fraction of $\ell_i \to \ell_j\gamma$ is given by [63]

$$\mathrm{Br}(\ell_i \to \ell_j\gamma) \simeq \frac{1}{\Gamma_{\ell_i}} \frac{\alpha_e m_{\ell_i}^3}{1024\pi^4} (|\sigma_L|^2 + |\sigma_R|^2), \tag{3.5}$$

where m_{ℓ_i} and Γ_{ℓ_i} are the mass and total decay width of the lepton ℓ_i, while α_e is the electromagnetic fine-structure constant. The dominant contributions arise from Z' or χ exchange, and they are given by

$$\sigma_L \simeq \sum_{a=1,2} \left(\frac{m_{E_a}}{m_{Z'}^2} [\hat{g}^{Z'}_R]_{jE_a} [\hat{g}^{Z'}_L]_{E_a i} G_Z(x_a) + \frac{m_{E_a}}{4 m_\chi^2} [\hat{Y}^\chi_e]_{jE_a} [\hat{Y}^\chi_e]_{E_a i} G_S(y_a) \right) \tag{3.6}$$

and σ_R which is given by formally replacing $L \to R$ and $\hat{Y}^\chi_e \to (\hat{Y}^\chi_e)^\dagger$ in the above expression. Other contributions, involving the SM bosons or σ, only amount to subpercent corrections at our best fit points.

C. Wilson coefficients for $b \to s\ell^+\ell^-$

The Wilson coefficients defined in Eqs. (1.2) are given by

$$C_9^\ell = -\frac{\sqrt{2}}{4G_F}\frac{4\pi}{\alpha_e}\frac{1}{V_{tb}V_{ts}^*}\frac{1}{2m_{Z'}^2}[\hat{g}^{Z'}_{d_L}]_{23}[\hat{g}^{Z'}_{e_R}+\hat{g}^{Z'}_{e_L}]_{ii}, \quad (3.7)$$

$$C_{10}^\ell = -\frac{\sqrt{2}}{4G_F}\frac{4\pi}{\alpha_e}\frac{1}{V_{tb}V_{ts}^*}\frac{1}{2m_{Z'}^2}[\hat{g}^{Z'}_{d_L}]_{23}[\hat{g}^{Z'}_{e_R}-\hat{g}^{Z'}_{e_L}]_{ii}, \quad (3.8)$$

$$C_9^{\prime\ell} = -\frac{\sqrt{2}}{4G_F}\frac{4\pi}{\alpha_e}\frac{1}{V_{tb}V_{ts}^*}\frac{1}{2m_{Z'}^2}[\hat{g}^{Z'}_{d_R}]_{23}[\hat{g}^{Z'}_{e_R}+\hat{g}^{Z'}_{e_L}]_{ii}, \quad (3.9)$$

$$C_{10}^{\prime\ell} = -\frac{\sqrt{2}}{4G_F}\frac{4\pi}{\alpha_e}\frac{1}{V_{tb}V_{ts}^*}\frac{1}{2m_{Z'}^2}[\hat{g}^{Z'}_{d_R}]_{23}[\hat{g}^{Z'}_{e_R}-\hat{g}^{Z'}_{e_L}]_{ii}, \quad (3.10)$$

where $i = 1, 2, 3$ for $\ell = e, \mu, \tau$, respectively.

We refer to the recent two-dimensional analysis of Ref. [30] and adopt the best fit values of the Wilson coefficients as

$$\text{(I) } \mathrm{Re}C_9^\mu = -0.7 \pm 0.3, \quad \mathrm{Re}C_{10}^\mu = 0.4 \pm 0.25; \quad (3.11)$$

$$\text{(II) } \mathrm{Re}C_9^\mu = -1.04 \pm 0.24, \quad \mathrm{Re}C_9^{\prime\mu} = 0.48 \pm 0.30. \quad (3.12)$$

Note that the Z' should not introduce sizable Wilson coefficients for the electron because that would generically also induce a sizable violation of lepton flavor in $\mu \to e\gamma$. Although it has been pointed out that some flavor universal contributions seem to be favored [30,31,34], we do not discuss this possibility in the present paper.

D. Neutral meson mixing

There are strong constraints on neutral meson mixing [64,65]. The relevant effective Hamiltonian is given by

$$\mathcal{H}_{\mathrm{eff}}^{\Delta F=2} = \sum_{i,a} C_i^a Q_i^a, \quad (3.13)$$

where $(i, a) = $ (1, VLL), (1, VRR), (1, LR), (2, LR), (1, SLL), (2, SLL), (1, SRR), (2, SRR). The four-Fermi operators are defined as

$$Q_1^{\mathrm{VLL}} = (\bar{F}^\alpha\gamma_\mu P_L f^\alpha)(\bar{F}^\beta\gamma^\mu P_L f^\beta),$$
$$Q_1^{\mathrm{VRR}} = (\bar{F}^\alpha\gamma_\mu P_R f^\alpha)(\bar{F}^\beta\gamma^\mu P_R f^\beta), \quad (3.14)$$

$$Q_1^{\mathrm{LR}} = (\bar{F}^\alpha\gamma_\mu P_L f^\alpha)(\bar{F}^\beta\gamma^\mu P_R f^\beta),$$
$$Q_2^{\mathrm{LR}} = (\bar{F}^\alpha P_L f^\alpha)(\bar{F}^\beta P_R f^\beta), \quad (3.15)$$

$$Q_1^{\mathrm{SLL}} = (\bar{F}^\alpha P_L f^\alpha)(\bar{F}^\beta P_L f^\beta),$$
$$Q_2^{\mathrm{SLL}} = (\bar{F}^\alpha \sigma_{\mu\nu} P_L f^\alpha)(\bar{F}^\beta \sigma^{\mu\nu} P_L f^\beta), \quad (3.16)$$

$$Q_1^{\mathrm{SRR}} = (\bar{F}^\alpha P_R f^\alpha)(\bar{F}^\beta P_R f^\beta),$$
$$Q_2^{\mathrm{SRR}} = (\bar{F}^\alpha \sigma_{\mu\nu} P_R f^\alpha)(\bar{F}^\beta \sigma^{\mu\nu} P_R f^\beta). \quad (3.17)$$

Here, α and β are color indices, and $(F, f) = (b, d), (b, s), (s, d)$ or (c, u) for B_d-$\bar{B}_d$, B_s-$\bar{B}_s$, K-$\bar{K}$, or D-$\bar{D}$ mixing, respectively. We focus here on B_q-$\bar{B}_q$ $(q = d, s)$ mixing since these are the most relevant for the $b \to s\ell^+\ell^-$ anomalies.

The Wilson coefficients induced by Z' or neutral scalar exchange, including $\mathcal{O}(\alpha_s)$ QCD corrections, are given by [66]

$$C_1^{\mathrm{VLL}}(\mu) = \left[1 + \frac{\alpha_s}{4\pi}\left(-2\log\frac{m_{Z'}^2}{\mu^2} + \frac{11}{3}\right)\right]\frac{g_L^{Z'}g_L^{Z'}}{2m_{Z'}^2}, \quad (3.18)$$

$$C_1^{\mathrm{LR}}(\mu) = \left[1 + \frac{\alpha_s}{4\pi}\left(-\log\frac{m_{Z'}^2}{\mu^2} - \frac{1}{6}\right)\right]\frac{g_L^{Z'}g_R^{Z'}}{m_{Z'}^2} - \left(-\frac{3}{2}\frac{\alpha_s}{4\pi}\right)\frac{y_L^\chi y_R^\chi}{2m_\chi^2}, \quad (3.19)$$

$$C_2^{\mathrm{LR}}(\mu) = \frac{\alpha_s}{4\pi}\left(-6\log\frac{m_{Z'}^2}{\mu^2} - 1\right)\frac{g_L^{Z'}g_R^{Z'}}{m_{Z'}^2} - \left(1 - \frac{\alpha_s}{4\pi}\right)\frac{y_L^\chi y_R^\chi}{2m_\chi^2}, \quad (3.20)$$

$$C_1^{\mathrm{SLL}}(\mu) = -\left[1 + \frac{\alpha_s}{4\pi}\left(-3\log\frac{m_\chi^2}{\mu^2} + \frac{9}{2}\right)\right]\frac{y_L^\chi y_L^\chi}{4m_\chi^2}, \quad (3.21)$$

$$C_2^{\mathrm{SLL}}(\mu) = -\frac{\alpha_s}{4\pi}\left(-\frac{1}{12}\log\frac{m_\chi^2}{\mu^2} + \frac{1}{8}\right)\frac{y_L^\chi y_L^\chi}{4m_\chi^2}, \quad (3.22)$$

where

$$g_L^{Z'} = [\hat{g}^{Z'}_{d_L}]_{3k}, \quad g_R^{Z'} = [\hat{g}^{Z'}_{d_R}]_{3k}, \quad y_L^\chi = [\hat{Y}_d^\chi]_{3k}, \quad y_R^\chi = [\hat{Y}_d^\chi]^*_{k3}, \quad (3.23)$$

and $k = 1(2)$ for $B_{d(s)}$-$\bar{B}_{d(s)}$ mixing, respectively. The analogous Wilson coefficients C_1^{VRR} and $C_{1,2}^{\mathrm{SRR}}$ are obtained by formally replacing $L \to R$. The off-diagonal element of the $B_q (q = d, s)$ meson mass matrix is given by

$$M_{12}^*(B_q) = M_{12}^{\mathrm{SM}*}(B_q) + \frac{1}{2m_{B_q}}\sum_{i,a} C_i^a(\mu)\langle\bar{B}_q|Q_i^a(\mu)|B_q\rangle, \quad (3.24)$$

where the first term is the SM contribution and m_{B_q} is the meson's physical mass. The SM contribution for B_q-$\bar{B}_q$ mixing is given by

$$M_{12}^{\mathrm{SM}*}(B_q) = \frac{G_F^2}{12\pi^2}m_W^2(\lambda_t^{(q)})^2 S_0(x_t)\eta_B m_{B_q} f_{B_q}^2 \hat{B}_{B_q}. \quad (3.25)$$

Here, $\lambda_t^{(q)} = V_{tb}^* V_{tq}$, $S_0(x_t = m_t^2/M_W^2) \approx 2.32$ is the Inami-Lim loop function [67], $\eta_B = 0.55 \pm 0.01$ [68,69] quantifies the short distance radiative corrections, while f_{B_q} and

TABLE III. Numerical values of the operators $O_i^a \coloneqq \langle \bar{M}|Q_i^a|M\rangle/(2m_M)$ at $\mu_B = 1$ TeV. The corresponding right-right (RR) operators have the same values as the left-left (LL) operators.

	$O_1^{\rm VLL}(\mu_B)$	$O_1^{\rm LR}(\mu_B)$	$O_2^{\rm LR}(\mu_B)$	$O_1^{\rm SLL}(\mu_B)$	$O_2^{\rm SLL}(\mu_B)$
K-$\bar{K}$	0.00159	−0.159	0.261	−0.0761	−0.132
B_d-$\bar{B}_d$	0.0465	−0.186	0.241	−0.0909	−0.167
B_s-$\bar{B}_s$	0.0701	−0.264	0.338	−0.136	−0.252
D-$\bar{D}$	0.0162	−0.157	0.227	−0.0845	−0.152

$\hat{B}_{B_q}$ denote the corresponding decay constant and SM hadronic matrix element. The SM and necessary beyond the SM hadronic matrix elements are calculated by lattice collaborations, and their values at 1 TeV according to our own evaluation are listed in Table III. Values for K-$\bar{K}$ and D-$\bar{D}$ mixing are also listed for completeness. All hadronic matrix elements for Kaon oscillations and the value of $f_{B_q}^2 \hat{B}_{B_q}$ have been taken from Ref. [70], while those for $f_{B_q}^2 B_{B_q}^{(2\text{–}5)}$ and $B_D^{(1\text{–}5)}$ have been taken from Refs. [71,72] and Ref. [73], respectively. The QCD running between the respective lattice scales and $\mu = 1$ TeV has been calculated based on the anomalous dimensions shown in Ref. [74].

The observables for B_q-$\bar{B}_q$ mixing are defined as

$$\Delta M_d \coloneqq 2|M_{12}(B_d)|, \qquad S_{\psi K_s} \coloneqq \sin\left(\mathrm{Arg}[M_{12}(B_d)]\right), \tag{3.26}$$

$$\Delta M_s \coloneqq 2|M_{12}(B_s)|, \qquad S_{\psi\phi} \coloneqq -\sin\left(\mathrm{Arg}[M_{12}(B_s)]\right). \tag{3.27}$$

The mass differences ΔM_d and ΔM_s are measured with high accuracy, and theoretical uncertainties are prevailing. The dominant theoretical uncertainties arise from the CKM elements, hadronic matrix elements, and next-to-leading order QCD corrections. Altogether we find 15.6% (14.1%) relative uncertainty for $\Delta M_d (\Delta M_s)$. Note that, unlike the analyses in e.g., Refs. [65,75], we cannot reduce the uncertainties by assuming the exact unitarity of the CKM matrix here, simply because CKM unitarity is not guaranteed in our model. We therefore have to rely on the measured CKM matrix elements and their respective errors. Despite the possible CKM nonunitarity, we still use formulas for the SM contributions which are obtained under the implicit assumption of exact CKM unitarity (i.e., a working Glashow-Iliopoulos-Maiani mechanism). This adds some additional theoretical uncertainty which is hard to quantify. As the CKM matrix at our fit points is still approximately unitary to the observed degree, we neglect this additional uncertainty.

We find that the pattern (II) of the Wilson coefficients for $b \to s\ell^+\ell^-$ [cf. Eq. (3.11)] is disfavored because this would cause large Z' contributions to ΔM_s. A large negative contribution $\mathrm{Re}C_9^\mu$ together with a positive $\mathrm{Re}C_9'^\mu$ requires a relative sign difference between $\mathrm{Re}[g_{d_L}^{Z'}]_{23}$ and $\mathrm{Re}[g_{d_R}^{Z'}]_{23}$. Since the hadronic matrix element $O_1^{\rm LR}$ is sizable and negative, this would imply a large and positive left-right contribution to ΔM_s. However, as the current SM prediction is already larger than the experimental value, the Z' coupling with $\mathrm{Re}C_9'^\mu$ is strongly disfavored. For this reason, we could not find any good fit points for the pattern (II).

E. Neutrino trident production

The so-called neutrino trident production $\nu_\mu \to \nu_\mu \mu\mu$ off a nucleus is a rare process that has been observed at a rate consistent with SM expectations [76–78]. This process can also be mediated by Z' exchange and therefore constitutes an important bound on NP scenarios [42,79–83]. The ratio of the cross section including NP at the CCFR experiment can be estimated as [83]

$$\frac{\sigma_{\rm CCFR}}{\sigma_{\rm CCFR}^{\rm SM}} \simeq \frac{(1+4s_W^2+\Delta g_{\mu\mu\mu\mu}^V)^2 + 1.13(1-\Delta g_{\mu\mu\mu\mu}^A)^2}{(1+4s_W^2)^2+1.13}, \tag{3.28}$$

with a current experimental limit of $\sigma/\sigma^{\rm SM} = 0.82 \pm 0.28$ at 95% C.L. The effective four-Fermi couplings $\Delta g_{\mu\mu\mu\mu}^{V,A}$ in our model are given by

$$\Delta g_{\mu\mu\mu\mu}^{V,A} = \frac{1}{\sqrt{2} G_F m_{Z'}^2} [g_\nu^{Z'}]_{\nu_\mu \nu_\mu} ([g_{e_R}^{Z'}]_{22} \pm [g_{e_L}^{Z'}]_{22}), \tag{3.29}$$

where $[g_\nu^{Z'}]_{\nu_\mu \nu_\mu}$ is defined in the flavor basis,

$$g_\nu^{Z'} = g' U_{e_L}^\dagger Q'_{n_L} U_{e_L}. \tag{3.30}$$

This constraint is particularly relevant for light Z''s and quickly becomes insensitive to NP once the Z' is heavier than a few 100 GeV.

F. Gauge kinetic mixing

A potentially light Z' boson can experience sizable gauge kinetic mixing with the $\mathrm{U}(1)_\mathrm{Y}$ gauge boson, namely the Z of the SM. The Z-Z' mixing parameter ε is estimated as

$$\varepsilon \simeq \frac{g_Y g'}{6\pi^2} \log\left(\frac{m_E^2}{m_L^2} \frac{m_Q^2 m_D^2}{m_U^4}\right), \tag{3.31}$$

where m_F ($F = L, E, Q, U, D$) are the VL mass terms for the VL fermions and g_Y is the $\mathrm{U}(1)_\mathrm{Y}$ gauge coupling constant. Current experimental limits are summarized in Ref. [84]. Values of $\varepsilon \sim 0.05$ cannot be ruled out if the Z' is heavier than a few hundred giga-electron-volts.

TABLE IV. Values of selected observables at the best fit points A and B.

Parameters	Point A	Point B	Remark
χ^2	25.1	24.9	$N_{\rm inp} = 65$, $N_{\rm obs} = 98$
g'	0.266	0.306	$\lesssim 0.35$ for $\Lambda_{g'} = 10^{16}$ GeV
(v_Φ, v_ϕ) [TeV]	(1.31, 4.36)	(0.872, 2.92)	
Observables	Point A	Point B	Data
$\Delta a_\mu \times 10^9$	2.56	2.43	2.68(76) [1]
$\mathrm{Br}(\mu \to e\gamma) \times 10^{13}$	3.58	2.10	<4.2 (90% C.L.) [1]
$\mathrm{Br}(\tau \to \mu\gamma) \times 10^8$	1.96×10^{-5}	4.91×10^{-2}	<4.4 (90% C.L.) [1]
$\mathrm{Br}(\tau \to \mu\mu\mu) \times 10^8$	3.03×10^{-5}	7.42×10^{-3}	<2.1 (90% C.L.) [1]
$\mathrm{Re}C_9^\mu$	−0.725	−0.571	−0.7(3) [30]
$\mathrm{Re}C_{10}^\mu$	0.320	0.316	0.4(2) [30]
ΔM_d [ps^{-1}]	0.612	0.599	0.507(81) [1]
ΔM_s [ps^{-1}]	19.4	19.8	17.8(2.5) [1]
$S_{\psi K_s}$	0.688	0.686	0.695(19) [85]
$S_{\psi\phi}$	0.0374	0.0363	0.021(31) [85]

IV. RESULTS

A. χ^2 Fitting

We minimize the χ^2 function

$$\chi^2(x) \coloneqq \sum_I \frac{(y_I(x) - y_I^0)^2}{\sigma_I^2}, \qquad (4.1)$$

where x is a point in the parameter space, while $y_I(x)$ is the value of observable I with central value y_I^0 and uncertainty σ_I. Observables we fit to include the SM fermion masses, CKM matrix element absolute values and relative phases, SM particle branching fractions (including flavor violating decays), neutral meson mixing, Δa_μ, $C_{9,10}^{(\prime)l}$, and some others. In total, we consider 98 observables, and they are all listed in Appendixes B and C.

In total, there are 65 input parameters represented by x in our analysis. The bosonic sector has five parameters,

$$m_{Z'}, \quad v_\phi, \quad g', \quad \lambda_\chi, \quad \lambda_\sigma, \qquad (4.2)$$

which are the Z' mass, the VEV of ϕ, the U(1)$'$ gauge coupling constant, and the effective quartic couplings defined in Eq. (2.11), respectively. All other parameters are Yukawa couplings as defined in Eqs. (2.2)–(2.5). For the neutrino sector, we only consider the couplings $\lambda_n^{(\prime)}$ and λ_V^N which are relevant for the new tera-electron-volt–scale state. The remaining Yukawa couplings y_{ij}^n, λ_j^N as well as the heavy Majorana masses are not varied in our analysis because these are relevant only for the details of masses and mixings of the SM neutrinos (and the RH Majorana neutrinos). Thus, effects suppressed by the Majorana masses are neglected. We expect that the number of parameters in the neutrino sector is sufficient to explain the observed neutrino mass squared differences and the PMNS matrix without changing any observables studied in our analysis. We assume that all Yukawa couplings are real except for $y_{13}^{u,d}$ and $y_{31}^{u,d}$. Altogether, there are then 60 real parameters for the Yukawa couplings. All Yukawa couplings and effective quartic coupling values are restricted to be smaller than unity. Furthermore, as already discussed at the end of Sec. II, $g' < 0.35$ is required so that the gauge coupling g' stays perturbative up to approximately 10^{16} GeV.

B. Best fit points

We find two best fit points A and B with $\chi^2 = 25.1$ and $\chi^2 = 24.9$, respectively, for $98 - 65 = 33$ d.o.f. The values of all observables and the corresponding input parameters are listed in Appendixes B and C. The values of selected observables are shown in Table IV. Masses and dominant decay modes of new particles are summarized in Tables V and VI.

TABLE V. Masses, total widths, and branching fractions (Br) at point A. Decay 1 (2) denotes the (next to) dominant decay mode.

	Mass (GeV)	Width (GeV)	Decay 1	Br	Decay 2	Br
Z'	494.7	0.7723	$\mu\mu$	0.4058	$\nu\nu$	0.3529
χ	1314	2.290	N_1N_1	0.2934	$E_1\mu$	0.1477
σ	4345	3.667	U_1t	0.2516	D_1b	0.2476
E_1	267.2	$2. \times 10^{-6}$	$h\mu$	0.6774	$Z\mu$	0.1693
N_1	359.2	0.5505	WE_1	1.000	$W\mu$	0.0000
E_2	442.4	1.783	ZE_1	0.8646	WN_1	0.1084
N_2	4357	0.0019	$W\mu$	0.3745	$Z\nu$	0.1872
D_1	2120	1.535	$Z'b$	0.4514	Wt	0.3629
U_1	2120	1.538	$Z't$	0.4552	ht	0.1840
D_2	2947	1.029	WU_1	0.4983	ZD_1	0.2493
U_2	4252	1.042	WD_1	0.4901	ZU_1	0.2450

At both best fit points, deviations from the SM in Δa_μ and C_9^μ, C_{10}^μ are explained by NP contributions. Besides a dominant positive loop contribution to Δa_μ involving the Z', there is a slight cancellation from a negative contribution of the scalar χ at both points. All observables are fit within their 2σ ranges at both points, except for Δa_e, which cannot be explained in the SM either; see e.g., Refs. [86–92]. We could not find points which have Δa_e near the experimental value while LFV processes, especially $\mathrm{Br}(\mu \to e\gamma)$, are sufficiently suppressed. The only observables with pulls exceeding 1σ are $\mathrm{Br}(\mu \to e\gamma)$, ΔM_{B_d}, and some absolute values of CKM elements. Interestingly, the NP correction to B_d-$\bar{B}_d$ from Z'-boson exchange is sizable, while B_s-$\bar{B}_s$ mixing is within its 1σ range (taking into account the experimental uncertainties for $|V_{ts}|$ and $|V_{tb}|$).

The 3×3 CKM matrix of the SM families, $[V_{\mathrm{CKM}}]_{ij} \coloneqq [\hat{V}_{\mathrm{CKM}}]_{ij}$, is almost unitary with deviations smaller than

$$|V_{\mathrm{CKM}}^\dagger V_{\mathrm{CKM}} - \mathbb{1}_3| \lesssim 5.1(1.9) \times 10^{-8}, \qquad (4.3)$$

at the point A(B). The full 5×5 CKM matrices at the best fit points are shown in Appendixes B and C.

C. Phenomenology

We now discuss the phenomenology of this model at the best fit points. Since the Z' gauge boson and the VL leptons are comparatively light, constraints from direct searches at the LHC and from muon flavor physics are both very important.

1. *Z' physics*

The Z'-boson mass is 494.7(377.1) GeV at the best fit point A(B). There are strong limits on such a comparatively light Z' from direct searches at the LHC. Other important constraints on the Z' mass arise from the so-called neutrino trident production as well as from gauge kinetic mixing with the Z boson. However, we will see that, despite its relative lightness, the Z' boson is still sufficiently heavy to evade these bounds.

General LHC limits on Z' bosons responsible for $b \to s\ell^+\ell^-$ anomalies are studied in Refs. [93,94]. The most stringent bound from the LHC on our model comes from resonance searches in the dimuon channel,

$$pp \to Z' \to \mu^+\mu^-. \qquad (4.4)$$

This is particularly pronounced in our model, as the dominant decay modes of the Z' are $Z' \to \mu^+\mu^-$ and $Z' \to \nu\nu$, as shown in Tables V and VI. Exclusion bounds are given in Ref. [95] based on 139 fb^{-1} of data. We have calculated the fiducial cross section, as defined in Ref. [95], using MadGraph5_2_6_5 [96] based on a UFO [97] model file generated with FeynRules_2_3_32 [96,98]. The fiducial cross section is 0.477(0.482) fb at the point A(B).

TABLE VI. Masses, total widths, and branching fractions (Br) at point B. Decay 1 (2) denotes the (next to) dominant decay mode.

	Mass (GeV)	Width (GeV)	Decay 1	Br	Decay 2	Br
Z'	377.1	0.1112	$\mu\mu$	0.5193	$\nu\nu$	0.4793
χ	135.4	$9. \times 10^{-9}$	$\mu\mu$	0.8094	bs	0.0945
σ	2915	5.575	E_2E_2	0.2688	E_1E_1	0.1486
N_1	280.2	0.0003	$W\mu$	0.5232	$Z\nu$	0.2578
E_1	571.9	0.4464	$\chi\mu$	0.5495	$Z'\mu$	0.3684
N_2	580.7	0.4718	$\chi\nu$	0.5427	$Z'\nu$	0.3741
E_2	1174	23.07	WN_2	0.4698	ZE_1	0.2340
D_1	1548	0.3587	$Z's$	0.2889	χs	0.2874
U_1	1548	0.3594	$Z'c$	0.2833	χc	0.2818
D_2	2902	0.1854	$Z'b$	0.4448	χb	0.4432
U_2	2915	0.0441	WD_1	0.3897	hU_1	0.1969

This is roughly 4 (6) times smaller than the experimental limit for the respective Z' masses [95]. The production cross sections are very suppressed because the Z' couplings to the SM quarks are at most $\mathcal{O}(10^{-3})$. We stress that both of our fit points realize solutions to the observed anomalies where the dimuon coupling of the Z' is maximal, while the $Z'bs$ coupling is minimal.

The ratio of neutrino trident production at CCFR is 1.014 (1.006), very close to the SM and well in agreement with the experimental constraints. The gauge kinetic $Z - Z'$ mixing at the best fit points is estimated as $\varepsilon \sim 2.0 \times 10^{-3}$ (7.6×10^{-4}) and therefore also well below the experimental bounds.

2. *Lepton flavor physics*

In general, a variety of charged LFV processes is present in this model. As discussed in Sec. III B, loops involving Z' or the scalar χ together with VL leptons can lead to chirally enhanced contributions to $\ell_1 \to \ell_2\gamma$ processes. Furthermore, also LFV tree-level Z' exchange is possible and could induce $\ell \to \ell_1\ell_2\ell_3$ processes. The LFV couplings here arise from the mixing between the SM families and the VL family. Although these LFV processes exist in principle, they can easily be suppressed by certain patterns of Yukawa couplings such as $\lambda_2^{L,E} \gg \lambda_3^{L,E}$, $\lambda_1^{L,E}$ and gauge eigenstates which are otherwise closely aligned with the mass eigenstates. Specific textures of the Yukawa couplings like this could be explained by flavor symmetries.

At the best fit points, we find that from all possible charged LFV processes only $\mathrm{Br}(\mu \to e\gamma)$ is close to its experimental upper bound. Just like for Δa_μ, the dominant contribution to $\mu \to e\gamma$ originates from the chirally enhanced Z' loop with heavy leptons, with an $\mathcal{O}(10\%)$ cancellation arising from the χ-loop contribution.

The SM-boson decays may in general also be affected by mixing effects. Models with VL leptons mixing to the SM families often affect the LFV Higgs-boson decays such as $h \to \mu\tau$, and also changes in the rates of lepton flavor conserving decays, see e.g., Refs. [40,46,99]. However, in the generic parameter regions of our best fit points, there is no significant contribution from the mixing to these processes. As analytically demonstrated in Appendix A, this comes about because mixing between the SM families and the VL family is only induced by the $\mathrm{U}(1)'$-breaking scalar Φ instead of the Higgs boson. Thus, the Higgs-boson decays to SM generations are very much aligned with the SM. The same is true for the couplings of the Z boson which are very SM-like for the three SM generations.

3. Quark flavor physics

There is much literature discussing the correlation between the $b \to s\ell^+\ell^-$ anomalies and B_s-$\bar{B}_s$ mixing since these are induced by common operators; see e.g., Ref. [65]. The recent lattice results [70,72,100,101] imply that the SM contribution to ΔM_s is slightly larger than the experimental central value. The Z'-boson contribution to C_9^μ also gives a constructive correction to ΔM_s, so ΔM_s tends to deviate from the central value even more. However, the theoretical uncertainties are large, so this is currently not the tightest bound on the model.

We stress that, unlike the case for the charged leptons, all of the SM quark families must mix in the up and/or down quark sectors to explain the observed CKM matrix. This implies that there can be sizable NP contributions not only to B_s-$\bar{B}_s$ mixing—as commonly considered in the context of $b \to s\ell^+\ell^-$ anomalies—but also to B_d-$\bar{B}_d$, K-$\bar{K}$, and D-$\bar{D}$ mixing. Even if the Z' contributions to the latter are much smaller at face value than those to B_s-$\bar{B}_s$ mixing, the NP effects can still be significant, as also the SM contributions are further suppressed. This is demonstrated by our two best fit points where $\Delta M_d \sim 0.6\ \mathrm{ps}^{-1}$ is about 1σ larger than the experimentally observed value.

In general, we note that future, more precise determinations and overconstraining of the CKM elements gives very important tests for this model, complementary to other probes. Currently, there are several tensions with current data at the approximately 1σ level, cf. the tables in Appendixes B and C. Very recently, it has been argued that experiments may be in favor of CKM nonunitarity [102]. While it has to be carefully evaluated whether these hints hold up, we remark that our model is in principle very well equipped to explain such effects.

4. Collider signals of vectorlike fermions

The VL leptons tend to be light in order to explain Δa_μ. If the VL lepton is lighter than both the Z' boson and the scalar χ, as for example the lightest charged VL lepton E_1 at point A, it decays to a SM boson and a SM lepton, as usually considered as a signal for VL leptons [103–109]. At point A, the lightest VL lepton E_1 is approximately a weak singlet, and it decays to $h\mu$, $Z\mu$, and $W\nu$ with branching fractions of about 70%, 15%, and 15%, respectively. Given the analysis of Ref. [104], which is based on LHC run 1 data, the VL lepton at point A is not excluded. The LHC run 2 data were studied to search for a weak doublet VL lepton decaying to a SM boson and a tau lepton in Ref. [105]. The limit from this analysis is expected to be much weaker for a weak singlet VL lepton decaying to a muon and a SM boson. We hope that a VL lepton of this type will be searched for by a dedicated analysis based on LHC run 2 data.

In contrast, if the VL lepton is heavier than χ and/or Z', it tends to decay to them. For example, at point B, the lightest charged VL lepton E_1 predominantly decays to $\chi\mu$, and χ subsequently decays to dimuons or ditops, if kinematically allowed. An expected signal in this case is

$$pp \to E_1^+ E_1^- \to \mu^+\chi(\to \mu^+\mu^-) + \mu^-\chi(\to \mu^+\mu^-). \tag{4.5}$$

This signal is very clean with six muons and two pairs of dimuon resonances. Furthermore, (E_1, N_2) forms approximately a weak doublet, such that the pair production cross section is enhanced compared to the weak singlet case.

In addition to the lightest VL leptons, also the heavier VL leptons produce distinctive signals. These tend to decay to the lighter VL leptons, with the emission of a large number of light leptons. For instance, at the point A, the pair produced E_2 gives a dramatic signal,

$$pp \to E_2^+ E_2^- \to ZE_1^+ + ZE_1^- \to Z\mu^+(h/Z) + Z\mu^-(h/Z), \tag{4.6}$$

with up to ten leptons in the final state. These high-multiplicity lepton signals could provide a strong probe of this model.

The VL quarks are also detectable at the LHC. Limits for VL quarks are studied in Refs. [110,111] using the LHC run2 data, but the decay patterns of the VL quarks in our model are much more complicated than the ones assumed in these analyses. Furthermore, even the lightest VL quark has a mass of 2.1(1.5) TeV at the point A(B), which is heavier than the experimental lower bound of 1.4 TeV [111]. In fact, the VL quarks are typically much heavier than both the Z' or χ. They decay to a Z' or χ and a SM quark with comparable branching fractions. The signal from the pair production of the VL quarks is thus two (top) jets together with two resonance signatures. An interesting signal arises again for the case in which a boson decays to dimuons,

$$pp \to Q\bar{Q} \to \mathrm{jet}Z'(\to \mu^+\mu^-) + \mathrm{jet}Z'(\to \mu^+\mu^-), \tag{4.7}$$

where Q is one of the VL quarks. Again, this should give very clean signals at the LHC. Finally, note that the VL quarks can also induce missing energy signals like squarks when both of a pair of produced VL quarks decay as $Q \to \mathrm{jet}Z'(\to \nu\nu)$.

V. CONCLUSION

We have studied a model with a complete fourth family of vectorlike fermions which are charged under a new $\mathrm{U}(1)'$ gauge symmetry. We find parameter points at which the experimentally observed deviations in the muon anomalous magnetic moment Δa_μ and $b \to s\ell^+\ell^-$ processes are explained without altering too much those observables that are consistent with the SM predictions.

The model can be embedded into more unified pictures, like grand unification and/or string models, and it has a straightforward supersymmetric extension. To this extent, it is important that all observables can be consistently explained with small $\mathrm{U}(1)'$ gauge coupling g', such that the coupling remains perturbative up to a typical GUT scale approximately 10^{16} GeV. An important consequence of demanding a resolution to Δa_μ is that the $\mathrm{U}(1)'$ charge assignment for the VL family is not compatible with an SU(5) GUT, but instead with a Pati-Salam gauge symmetry.

In the present paper, we have displayed two good fit points which demonstrate that this model can explain the muon anomalies without spoiling other observables. The explanation of the anomalies is correlated with other beyond the Standard Model predictions for observables including lepton flavor violation, neutral meson mixing, deviations from the SM CKM matrix, and rare meson decays. The CKM matrix in the model easily fulfills unitarity at the currently observed level but is in general nonunitary. Hints for CKM nonunitarity found in a recent analysis could thus easily be accommodated and would give strong motivation to further consider this model. Distinct signals at the LHC in $Z' \to \mu\mu$ and pair production of VL leptons and VL quarks together with clean and distinct (resonant) multilepton final states are predicted and provide important means to test the considered parameter space.

In general, there are upper bounds on the VL fermions in order to explain the muon anomalies in this model. It will thus be interesting to have a global study of how wide a parameter space is consistent with current and future experiments. More details of our analysis and more global features of this model will be discussed in an upcoming paper.

ACKNOWLEDGMENTS

The authors are grateful to R. Dermisek for useful discussions about this vectorlike model. The work of J. K. and S. R. is supported in part by the U.S. Department of Energy under Award No. DE-SC0011726. The work of J. K. is supported in part by the Grant-in-Aid for Scientific Research from the Ministry of Education, Science, Sports and Culture, Japan, Grant No. 18K13534. The work of A. T. was partly supported by a postdoctoral fellowship of the German Academic Exchange Service. A. T. is grateful to the Physics Department of Ohio State University and Centro de Física Teórica de Partículas at Instituto Superior Técnico, Lisbon, for hospitality during parts of this work.

APPENDIX A: ANALYTICAL ANALYSIS

We discuss the analytical expressions for the couplings in the mass basis. We diagonalize the mass matrix in Eq. (2.6) perturbatively by exploiting $m_\ell \ll \tilde{M}_\ell$, where m_ℓ and $\tilde{M}_\ell$ represent the typical mass scales of charged leptons and VL leptons, respectively.

Let us define the unitary matrices,

$$U_L^0 \coloneqq \begin{pmatrix} \boldsymbol{z}_{L_j} & \boldsymbol{n}_L & \mathbf{0} \\ 0_j & 0 & 1 \end{pmatrix}, \quad U_R^0 \coloneqq \begin{pmatrix} \boldsymbol{z}_{E_j} & \boldsymbol{n}_E & \mathbf{0} \\ 0_j & 0 & 1 \end{pmatrix}, \tag{A1}$$

with the four-component vectors

$$\boldsymbol{n}_L \coloneqq \frac{1}{\tilde{M}_L} \begin{pmatrix} \lambda_i^{L*} v_\Phi \\ \lambda_V^{L*} v_\phi \end{pmatrix}, \qquad \boldsymbol{n}_E \coloneqq \frac{1}{\tilde{M}_E} \begin{pmatrix} \lambda_i^{E} v_\Phi \\ \lambda_V^{E} v_\phi \end{pmatrix}, \tag{A2}$$

and $\boldsymbol{z}_{E_i}$, $\boldsymbol{z}_{L_i}$, which obey the conditions

$$\boldsymbol{z}_{L_i}^\dagger \boldsymbol{n}_L = \boldsymbol{z}_{E_i}^\dagger \boldsymbol{n}_E = 0, \qquad \boldsymbol{z}_{L_i}^\dagger \boldsymbol{z}_{L_j} = \boldsymbol{z}_{E_i}^\dagger \boldsymbol{z}_{E_j} = \delta_{ij}. \tag{A3}$$

Here,

$$\tilde{M}_L \coloneqq \sqrt{\sum_{i=1}^{3} |\lambda_i^L|^2 v_\Phi^2 + |\lambda_V^L|^2 v_\phi^2},$$
$$\tilde{M}_E \coloneqq \sqrt{\sum_{i=1}^{3} |\lambda_i^E|^2 v_\Phi^2 + |\lambda_V^E|^2 v_\phi^2}. \tag{A4}$$

The rotated mass matrix is

$$\tilde{\mathcal{M}}^e \coloneqq U_R^{0\dagger} \mathcal{M}^e U_L^0 = \begin{pmatrix} \tilde{y}_{ij}^e v_H & \tilde{y}_{R_i} v_H & 0_i \\ \tilde{y}_{L_j} v_H & \tilde{\lambda}_e v_H & \tilde{M}_E \\ 0_j & \tilde{M}_L & \lambda_e' v_H \end{pmatrix}, \tag{A5}$$

where

$$\tilde{y}_{ij}^e \coloneqq \boldsymbol{z}_{E_i}^\dagger \hat{y}^e \boldsymbol{z}_{L_j}, \qquad \tilde{y}_{R_i} \coloneqq \boldsymbol{z}_{E_i}^\dagger \hat{y}^e \boldsymbol{n}_L,$$
$$\tilde{y}_{L_j} \coloneqq \boldsymbol{n}_E^\dagger \hat{y}^e \boldsymbol{z}_{L_j}, \qquad \tilde{\lambda}_e \coloneqq \boldsymbol{n}_E^\dagger \hat{y}^e \boldsymbol{n}_L, \tag{A6}$$

with

$$\hat{y}^e \coloneqq \begin{pmatrix} y_{ij}^e & 0_i \\ 0_j & \lambda_e \end{pmatrix}. \tag{A7}$$

In this matrix, $\tilde{y}^e_{ij}$, $\tilde{y}_{L_i}$, $\tilde{y}_{R_i}$, and $\tilde{\lambda}_e$ are of the order $\mathcal{O}(m_\ell/v_H)$, while $\tilde{M}_L$, $\tilde{M}_E \sim \tilde{M}_\ell$. Here, we assume $\lambda_e v_H \lesssim m_\mu$, in order for the muon mass to be explained without fine-tuning. Note that $\lambda'_e v_H$ can be as large as the VL lepton masses if $\lambda'_e \sim 1$ and the VL leptons are lighter than approximately 500 GeV. Hence, it cannot be treated as an expansion parameter in general.

Since the vectors $z'_{L_i} = [u_L]_{ij} z_{L_j}$ and $z'_{E_i} = [u_E]_{ij} z_{E_j}$, for arbitrary 3×3 unitary matrices u_L and u_E, also satisfy the conditions in Eq. (A3), we can always find a set of vectors z_{L_i}, z_{E_i} that diagonalize the SM Yukawa matrices, $\tilde{y}^e_{ij} = \mathrm{diag}(y^e_1, y^e_2, y^e_3)$. The mass matrix for the SM families then is almost diagonal except for the mixing with the VL family induced by $\tilde{y}_L$ and $\tilde{y}_R$. In order to explain the muon anomalies, there should be a sizable mixing among the muon and the VL leptons, while the mixing with the electron and tau can be suppressed in order to avoid lepton flavor violations which are strongly constrained by experiments. The simplest way to achieve this is by imposing the hierarchy $\lambda^{L,E}_2 \gg \lambda^{L,E}_{1,3}$. In this case, $\tilde{y}_{L_i}$, $\tilde{y}_{R_i} \sim m_\mu/v_H$ is expected.

We can show that the unitary matrices

$$U^1_L = \mathbb{1}_5 + \frac{1}{\tilde{M}_E}\begin{pmatrix} 0_{ij} & -\lambda'_e \tilde{y}^*_{L_i} v^2_H/\tilde{M}_L & \tilde{y}^*_{L_i} v_H \\ \lambda'_e \tilde{y}_{L_j} v^2_H/\tilde{M}_L & 0 & 0 \\ -\tilde{y}_{L_j} v_H & 0 & 0 \end{pmatrix} + \mathcal{O}\left(\frac{m^2_\ell}{\tilde{M}^2_\ell}\right), \tag{A8}$$

$$U^1_R = \mathbb{1}_5 + \frac{1}{\tilde{M}_L}\begin{pmatrix} 0_{ij} & -\lambda'_e \tilde{y}_{R_i} v^2_H/\tilde{M}_E & \tilde{y}_{R_i} v_H \\ \lambda'_e \tilde{y}^*_{R_i} v^2_H/\tilde{M}_E & 0 & 0 \\ -\tilde{y}^*_{R_j} v_H & 0 & 0 \end{pmatrix} + \mathcal{O}\left(\frac{m^2_\ell}{\tilde{M}^2_\ell}\right), \tag{A9}$$

block diagonalize the mass matrix as

$$U^{1\dagger}_R \tilde{\mathcal{M}}^e U^1_L = \mathrm{diag}\left(\tilde{y}^e_{ij} v_H + \tilde{y}_{R_i}\tilde{y}_{L_j}\frac{v^2_H}{\tilde{M}_L\tilde{M}_E}\lambda'_e v_H + \mathcal{O}\left(\frac{m^3_\ell}{\tilde{M}^2_\ell}\right), \begin{pmatrix} \tilde{\lambda}_e v_H & \tilde{M}_E \\ \tilde{M}_L & \lambda'_e v_H \end{pmatrix}\right). \tag{A10}$$

Here, higher order corrections for the heavy states have been neglected. The perturbative corrections to the mass matrix of the SM families are estimated as

$$\tilde{y}_{R_i}\tilde{y}_{L_j}\frac{v^2_H}{\tilde{M}_L\tilde{M}_E}\lambda'_e v_H \sim \frac{m^2_\mu}{\tilde{M}^2_\ell}\lambda'_e v_H = 2.2\times 10^{-5}\,\mathrm{GeV}\times\left(\frac{\lambda'_e v_H}{174\,\mathrm{GeV}}\right)\left(\frac{300\,\mathrm{GeV}}{\tilde{M}_\ell}\right)^2. \tag{A11}$$

For typical parameters, this is much smaller than the electron mass. Finally, we define unitary matrices $U^2_{L,R} \coloneqq \mathrm{diag}(\mathbb{1}_3, u_{L,R})$ which diagonalize the mass matrix of the VL family,

$$u^\dagger_R \begin{pmatrix} \tilde{\lambda}_e v_H & \tilde{M}_E \\ \tilde{M}_L & \lambda'_e v_H \end{pmatrix} u_L = \mathrm{diag}(m_{E_1}, m_{E_2}). \tag{A12}$$

Altogether, the fields in the mass basis $\hat{e}_L$, $\hat{e}_R$ can be written as

$$e_L = U^e_L \hat{e}_L \coloneqq U^0_L U^1_L U^2_L \hat{e}_L, \quad e_R = U^e_R \hat{e}_R \coloneqq U^0_R U^1_R U^2_R \hat{e}_R. \tag{A13}$$

We can now use this in order to study the scalar and gauge-boson couplings in the mass basis. Using Eqs. (A1) and (A8), one can show that

$$[(U^e_R)^\dagger Y^h_e U^e_L]_{ij} = \tilde{y}^e_{ij} + 2\lambda'_e \frac{v^2_H}{\tilde{M}_L\tilde{M}_E}\tilde{y}_{R_i}\tilde{y}_{L_j} + \mathcal{O}\left(\frac{m^2_\ell}{\tilde{M}^2}\right), \tag{A14}$$

and

$$[(U^e_L)^\dagger P_{\bar{5}} U^e_L]_{ij} = \delta_{ij} + \mathcal{O}\left(\frac{m^2_\ell}{\tilde{M}^2}\right),$$
$$[(U^e_R)^\dagger P_5 U^e_R]_{ij} = \mathcal{O}\left(\frac{m^2_\ell}{\tilde{M}^2}\right). \tag{A15}$$

The sizes of the perturbative corrections are estimated as

$$\lambda'_e \frac{v^2_H}{\tilde{M}_L\tilde{M}_E}\tilde{y}_{R_i}\tilde{y}_{L_j} \sim \lambda'_e \frac{m^2_\mu}{\tilde{M}^2_\ell} = 1.2\times 10^{-7}\times\left(\frac{\lambda'_e}{1.0}\right)\left(\frac{300\ \mathrm{GeV}}{\tilde{M}_\ell}\right)^2, \tag{A16}$$

$$\frac{m^2_\ell}{\tilde{M}^2_\ell} \lesssim \frac{m^2_\tau}{\tilde{M}^2_\ell} = 3.5\times 10^{-5}\times\left(\frac{300\ \mathrm{GeV}}{\tilde{M}_\ell}\right)^2. \tag{A17}$$

Therefore, the Higgs-boson coupling matrix is effectively diagonalized simultaneously with the mass matrix, and the left-handed neutral current gauge interactions of the SM families in the mass basis are to good accuracy proportional to the identity. In principle, there are also right-handed current corrections of the Z-/W-boson couplings to the SM fermions which are tested by precision measurements of Z- and W-boson properties (see e.g., [1]) neutrino-nucleon scattering [61], and so on, but their size is too small to be testable by these experiments.

The quark sector mass matrices can be diagonalized in a completely analogous fashion with the same conclusions. A significant difference with respect to the lepton sector can arise due to the heavy top quark mass. The relevant expansion parameter of the perturbation then is $m_t/\tilde{M}_q$, which only becomes less than or approximately equal to 0.1 if VL quark masses exceed approximately 1.5 TeV. However, in particular, for the up-type quarks, we may alternatively assume a hierarchy of couplings, $\lambda_i^Q v_\Phi$, $\lambda_i^U v_\Phi \ll \lambda_V^Q v_\phi$, $\lambda_V^U v_\phi$, which leads to the same conclusion.

APPENDIX B: DETAILS OF BEST FIT POINT A

1. Input parameters

The input parameters for the boson sector are

$$m_{Z'} = 494.696, \qquad v_\phi = 4356.63, \qquad g' = 0.266224, \qquad \lambda_\chi = 0.999975, \qquad \lambda_\sigma = 0.997241. \tag{B1}$$

The mass matrices are

$$M_e = \begin{pmatrix} -0.000486577 & 1.51118\times 10^{-6} & 1.99873\times 10^{-6} & 0 & -1.14426\times 10^{-6} \\ -1.98226\times 10^{-6} & -0.252886 & -0.00083412 & 0 & -179.053 \\ -5.17686\times 10^{-6} & 0.0000939331 & -1.74617 & 0 & -0.0268504 \\ 0 & 0 & 0 & -3.80325\times 10^{-7} & 276.103 \\ -0.0000358853 & 314.243 & -0.0370005 & -173.903 & -172.644 \end{pmatrix}, \tag{B2}$$

$$M_n = \begin{pmatrix} 0 & 0 & 0 & -0.816618 & -4356.63 \\ -0.0000358853 & 314.243 & -0.0370005 & -173.903 & 0.181800 \end{pmatrix}, \tag{B3}$$

$$M_u = \begin{pmatrix} -0.00210998 & 0.118413 & 1.44892\cdot e^{-0.0260154i} & 0 & -5.43376 \\ 0.00415738 & -0.612239 & 0.701898 & 0 & -0.168839 \\ 0.00168153\cdot e^{-1.90643i} & 0.132278 & -174.104 & 0 & -30.2055 \\ 0 & 0 & 0 & 0.0122855 & 4251.92 \\ -0.0725549 & -34.1972 & -344.810 & -2091.71 & -19.5774 \end{pmatrix}, \tag{B4}$$

$$M_d = \begin{pmatrix} -0.000539915 & -0.00944158 & 0.143965\cdot e^{1.62963i} & 0 & -0.465179 \\ 0.0105179 & 0.00784947 & -1.28759 & 0 & 8.33584 \\ 0.0124618\cdot e^{-1.98605} & 0.130429 & -2.58136 & 0 & 17.9036 \\ 0 & 0 & 0 & -0.000110584 & -2946.22 \\ -0.0725549 & -34.1972 & -344.810 & -2091.71 & 26.9254 \end{pmatrix}. \tag{B5}$$

Entries involving the three families of right-handed neutrinos are omitted here because these are suppressed by the huge Majorana mass and are irrelevant for our analysis; see Sec. IV.

2. Observables

In Tables VII–X, we show results for observables at the best fit point A. When quoted with reference, we have fitted the corresponding observable to experimental data. Otherwise, we have fitted to the tree-level SM prediction, which is indicated by “Ref” = “SM” Eight observables, namely the real and imaginary parts of $C_{9,10}^{e,(\prime)}$, are not shown because they are at most about 10^{-10}. More details on the fitting procedure will be given in our upcoming global analysis.

For convenience, we also state the extended CKM matrix at the best fit point A. It is given by

TABLE VII. Observables for charged leptons at point A.

Name	Value	Data	Uncertainty	Pull	Ref.
$m_e(m_Z)$ (GeV) $\times 10^4$	4.86579	4.86576	0.00049	0.068	[112]
$m_\mu(m_Z)$ (GeV)	0.102719	0.102719	0.000010	0.015	[112]
$m_\tau(m_Z)$ (GeV)	1.74617	1.74618	0.00017	0.029	[112]
$\mathrm{Br}(\mu \to e\nu\bar{\nu})$	0.99997	0.99997	0.00010	0.001	SM
$\mathrm{Br}(\mu^- \to e^-e^+e^-) \times 10^{13}$	0.000	0	7.8	0.000	[1]
$\mathrm{Br}(\mu \to e\gamma) \times 10^{13}$	3.581	0	3.3	1.093	[1]
$\mathrm{Br}(\tau \to e\nu\bar{\nu})$	0.178510	0.178510	0.000018	0.000	SM
$\mathrm{Br}(\tau \to \mu\nu\bar{\nu})$	0.173612	0.173612	0.000017	0.001	SM
$\mathrm{Br}(\tau^- \to e^-e^+e^-) \times 10^8$	0.000	0	2.1	0.000	[1]
$\mathrm{Br}(\tau^- \to e^-\mu^+e^-) \times 10^8$	0.000	0	1.2	0.000	[1]
$\mathrm{Br}(\tau^- \to \mu^-e^+\mu^-) \times 10^8$	0.000	0	1.3	0.000	[1]
$\mathrm{Br}(\tau^- \to \mu^-\mu^+\mu^-) \times 10^8$	3.0×10^{-5}	0	1.6	0.000	[1]
$\mathrm{Br}(\tau^- \to e^-\mu^+\mu^-) \times 10^8$	0.000	0	2.1	0.000	[1]
$\mathrm{Br}(\tau^- \to \mu^-e^+e^-) \times 10^8$	0.000	0	1.4	0.000	[1]
$\mathrm{Br}(\tau \to e\gamma) \times 10^8$	0.000	0	2.6	0.000	[1]
$\mathrm{Br}(\tau \to \mu\gamma) \times 10^8$	2.0×10^{-5}	0	3.4	0.000	[1]
$\Delta a_e \times 10^{13}$	-1.4×10^{-8}	−8.700	3.6	2.417	[86]
$\Delta a_\mu \times 10^9$	2.56	2.68	0.76	0.154	[1]

TABLE VIII. Observables for SM bosons at point A.

Name	Value	Data	Uncertainty	Pull	Ref.
$\mathrm{Br}(W^+ \to e^+\nu)$	0.10862	0.10862	0.00011	0.000	SM
$\mathrm{Br}(W^+ \to \mu^+\nu)$	0.10862	0.10862	0.00011	0.000	SM
$\mathrm{Br}(W^+ \to \tau^+\nu)$	0.10855	0.10855	0.00011	0.000	SM
$\mathrm{Br}(W \to \mathrm{had})$	0.652	0.666	0.025	0.550	SM
$\mathrm{Br}(W^+ \to c\bar{s})$	0.309	0.324	0.032	0.463	SM
$\mathrm{Br}(Z \to e^+e^-) \times 10^2$	3.333	3.333	0.0062	0.000	SM
$\mathrm{Br}(Z \to \mu^+\mu^-) \times 10^2$	3.333	3.333	0.0062	0.000	SM
$\mathrm{Br}(Z \to \tau^+\tau^-) \times 10^2$	3.326	3.326	0.0062	0.000	SM
$\mathrm{Br}(Z \to \mathrm{had})$	0.676	0.677	0.025	0.014	SM
$\mathrm{Br}(Z \to u\bar{u} + c\bar{c})/2$	0.1157	0.1157	0.0043	0.000	SM
$\mathrm{Br}(Z \to d\bar{d} + s\bar{s} + b\bar{b})/3$	0.1483	0.1483	0.0056	0.000	SM
$\mathrm{Br}(Z \to c\bar{c})$	0.1157	0.1157	0.0043	0.000	SM
$\mathrm{Br}(Z \to b\bar{b})$	0.1479	0.1479	0.0056	0.000	SM
$\mathrm{Br}(Z \to e\mu) \times 10^7$	0.000	0	4.6	0.000	[1]
$\mathrm{Br}(Z \to e\tau) \times 10^6$	0.000	0	6.0	0.000	[1]
$\mathrm{Br}(Z \to \mu\tau) \times 10^6$	0.000	0	7.3	0.000	[1]
A_e	0.1468	0.1468	0.0015	0.000	SM
A_μ	0.147	0.147	0.015	0.000	SM
A_τ	0.1468	0.1468	0.0015	0.000	SM
A_s	0.941	0.941	0.094	0.000	SM
A_c	0.6949	0.6949	0.0069	0.000	SM
A_b	0.9406	0.9406	0.0094	0.000	SM
$\mu_{\mu\mu}$	0.976	0	1.3	0.751	[1]
$\mu_{\tau\tau}$	0.981	1.12	0.23	0.607	[1]
μ_{bb}	0.841	0.950	0.22	0.495	[1]
$\mu_{\gamma\gamma}$	1.01	1.16	0.18	0.859	[1]

(Table continued)

TABLE VIII. *(Continued)*

Name	Value	Data	Uncertainty	Pull	Ref.
$\mathrm{Br}(h \to e^+e^-) \times 10^3$	4.8×10^{-6}	0	1.2	0.000	[1]
$\mathrm{Br}(h \to e\mu) \times 10^4$	0.000	0	2.1	0.000	[1]
$\mathrm{Br}(h \to e\tau) \times 10^3$	0.000	0	4.2	0.000	[1]
$\mathrm{Br}(h \to \mu\tau) \times 10^3$	0.000	0	8.7	0.000	[1]

TABLE IX. Quark masses and CKM matrix at point A.

Name	Value	Data	Uncertainty	Pull	Ref.
$m_u(m_Z)$ (GeV) $\times 10^3$	1.28	1.29	0.39	0.024	[112]
$m_c(m_Z)$ (GeV)	0.623	0.627	0.019	0.186	[112]
$m_t(m_Z)$ (GeV)	171.78	171.68	1.5	0.060	[112]
$m_d(m_Z)$ (GeV) $\times 10^3$	2.74	2.75	0.29	0.036	[112]
$m_s(m_Z)$ (GeV) $\times 10^3$	53.85	54.32	2.9	0.162	[112]
$m_b(m_Z)$ (GeV)	2.85	2.85	0.026	0.036	[112]
$\vert V_{ud}\vert$	0.97447	0.97420	0.00021	1.307	[1]
$\vert V_{us}\vert$	0.22447	0.22430	0.00050	0.338	[1]
$\vert V_{ub}\vert \times 10^3$	3.59	3.94	0.36	0.961	[1]
$\vert V_{cd}\vert$	0.2243	0.2180	0.0040	1.581	[1]
$\vert V_{cs}\vert$	0.974	0.997	0.017	1.374	[1]
$\vert V_{cb}\vert \times 10^2$	4.13	4.22	0.080	1.112	[1]
$\vert V_{td}\vert \times 10^3$	8.83	8.10	0.50	1.455	[1]
$\vert V_{ts}\vert \times 10^2$	4.05	3.94	0.23	0.485	[1]
$\vert V_{tb}\vert$	0.999	1.02	0.025	0.794	[1]
α	1.50	1.47	0.097	0.292	[1]
$\sin 2\beta$	0.698	0.691	0.017	0.440	[1]
γ	1.25	1.28	0.081	0.382	[1]

TABLE X. Observables for quarks at point A.

Name	Value	Data	Uncertainty	Pull	Ref.
ΔM_K (ps^{-1}) $\times 10^3$	4.616	5.293	2.2	0.312	[1]
$\epsilon_K \times 10^3$	2.24	2.23	0.21	0.038	[1]
ΔM_{B_d} (ps^{-1})	0.612	0.506	0.081	1.304	[1]
$S_{\psi K_s}$	0.688	0.695	0.019	0.368	[85]
ΔM_{B_s} (ps^{-1})	19.43	17.76	2.5	0.673	[1]
$S_{\psi\phi} \times 10^2$	3.740	2.100	3.1	0.529	[85]
$\vert x_{12}^D\vert \times 10^3$	5.3×10^{-5}	0	5.0	0.000	SM
$R_K^{\nu\nu}$	1.157	1.000	3.4	0.047	[113]
$R_{K^*}^{\nu\nu}$	1.158	1.000	3.4	0.046	[114]
$R_{B_d\to\mu\mu}$	0.860	1.509	1.4	0.457	[1,115,116]
$R_{B_s\to\mu\mu}$	0.862	0.750	0.16	0.709	[1,115,116]
Γ_t	1.49	1.41	0.17	0.485	[1]
$\mathrm{Br}(t \to Zq) \times 10^4$	0.000	0	3.0	0.000	[1]
$\mathrm{Br}(t \to Zu) \times 10^3$	0.000	0	1.5	0.000	[1]
$\mathrm{Br}(t \to Zc) \times 10^3$	0.000	0	1.3	0.000	[1]
$\mathrm{Re}C_9^\mu$	−0.725	−0.700	0.30	0.082	[30]

(Table continued)

TABLE X. *(Continued)*

Name	Value	Data	Uncertainty	Pull	Ref.
$\mathrm{Im}C_9^\mu$	-7.5×10^{-3}	0	0.10	0.075	[30]
$\mathrm{Re}C_{10}^\mu$	0.320	0.400	0.20	0.398	[30]
$\mathrm{Im}C_{10}^\mu$	3.3×10^{-3}	0	0.10	0.033	[30]
$\mathrm{Re}C_9^{\prime\mu}$	3.2×10^{-4}	0	0.10	0.003	[30]
$\mathrm{Im}C_9^{\prime\mu}$	-4.8×10^{-5}	0	0.10	0.000	[30]
$\mathrm{Re}C_{10}^{\prime\mu}$	-1.4×10^{-4}	0	0.10	0.001	[30]
$\mathrm{Im}C_{10}^{\prime\mu}$	2.1×10^{-5}	0	0.10	0.000	[30]
$\mathrm{Br}(B\to K\tau^+\tau^-)\times10^3$	1.2×10^{-4}	0	1.8	0.000	[117]

$$\hat{V}_{\mathrm{CKM}}=\begin{pmatrix} 0.974475 & 0.224469 & 0.003594\cdot e^{-1.25247i} & 0. & 0. \\ 0.224324\cdot e^{-3.14095i} & 0.973639 & 0.041311 & 0. & 0. \\ 0.008827\cdot e^{-0.385988i} & 0.040516\cdot e^{-3.12266i} & 0.999139 & 0.001086\cdot e^{1.21990i} & 0.000008\cdot e^{3.11582i} \\ 0.000010\cdot e^{2.75752i} & 0.000044\cdot e^{0.020825i} & 0.001084\cdot e^{-3.13970i} & 0.999902\cdot e^{1.22180i} & 0.013636\cdot e^{3.11681i} \\ 0.000003\cdot e^{2.77910i} & 0.000012\cdot e^{0.045064i} & 0.000287\cdot e^{-3.11555i} & 0.003122\cdot e^{1.24590i} & 0.000043\cdot e^{3.14091i} \end{pmatrix}. \tag{B6}$$

APPENDIX C: DETAILS OF BEST FIT POINT B

1. Input parameters

The input parameters for the boson sector are

$$m_{Z'}=377.090,\qquad v_\phi=2915.42,\qquad g'=0.305856,\qquad \lambda_\chi=0.155278,\qquad \lambda_\sigma=1.00000. \tag{C1}$$

The mass matrices are

$$M_e=\begin{pmatrix} 0.000486573 & 1.13824\times10^{-8} & 4.04521\times10^{-6} & 0 & -4.59216\times10^{-6} \\ 1.53811\times10^{-7} & -0.13295 & 0.0515715 & 0 & -360.594 \\ -0.0000578552 & 0.000174906 & -1.74549 & 0 & -0.142312 \\ 0 & 0 & 0 & -0.000263151 & 1099.09 \\ -1.26999\times10^{-6} & 337.256 & 0.0262194 & 472.383 & -174.012 \end{pmatrix}, \tag{C2}$$

$$M_n=\begin{pmatrix} 0 & 0 & 0 & 2.30874 & 280.271 \\ -1.26999\times10^{-6} & 337.256 & 0.0262194 & 472.383 & -16.3708 \end{pmatrix}, \tag{C3}$$

$$M_u=\begin{pmatrix} 0.0105038 & 0.494412 & 0.0290073\cdot e^{-0.532076i} & 0 & -0.30203 \\ -0.00667761 & -0.384139 & -0.110669 & 0 & 7.16682 \\ 0.450446\cdot e^{-1.77965i} & 8.95794 & -171.499 & 0 & -13.1159 \\ 0 & 0 & 0 & -0.00998379 & -2915.41 \\ -0.0540921 & -104.906 & 71.9157 & 1542.31 & -4.45885 \end{pmatrix}, \tag{C4}$$

$$M_d = \begin{pmatrix} -0.0111889 & 0.0531604 & 0.0128086\cdot e^{-0.481607i} & 0 & 0.0871297 \\ 0.00257029 & 0.00163007 & -0.0514564 & 0 & -1.52119 \\ 0.00240628\cdot e^{1.70936i} & 0.0308145 & -2.85816 & 0 & -65.9271 \\ 0 & 0 & 0 & 0.0101523 & 2901.32 \\ -0.0540921 & -104.906 & 71.9157 & 1542.31 & 3.43706 \end{pmatrix}. \quad \text{(C5)}$$

2. Observables

Tables XI–XIV show the observables at the best fit point B. The extended CKM matrix is given by

$$\hat{V}_{\mathrm{CKM}} = \begin{pmatrix} 0.974460 & 0.224533 & 0.003631\cdot e^{-1.21489i} & 0. & 0. \\ 0.224393\cdot e^{-3.14095i} & 0.973619 & 0.041392 & 0. & 0.000001\cdot e^{1.63235i} \\ 0.008717\cdot e^{-0.389908i} & 0.040627\cdot e^{-3.12277i} & 0.999136 & 0.000623\cdot e^{-1.59708i} & 0.000022\cdot e^{1.63174i} \\ 0.000005\cdot e^{-2.00027i} & 0.000025\cdot e^{1.54988i} & 0.000622\cdot e^{-1.61053i} & 0.999999\cdot e^{-0.066018i} & 0.000889\cdot e^{0.021202i} \\ 0.000002\cdot e^{-2.01687i} & 0.000011\cdot e^{1.52851i} & 0.000265\cdot e^{-1.63172i} & 0.001107\cdot e^{3.05439i} & 0.000001\cdot e^{-3.14158i} \end{pmatrix}. \quad \text{(C6)}$$

TABLE XI. Observables for charged leptons at point B.

Name	Value	Data	Uncertainty	Pull	Ref.
$m_e(m_Z)$ (GeV) $\times 10^4$	4.8658	4.8658	0.00049	0.007	[112]
$m_\mu(m_Z)$ (GeV)	0.102719	0.102719	0.000010	0.045	[112]
$m_\tau(m_Z)$ (GeV)	1.7462	1.7462	0.00017	0.039	[112]
$\mathrm{Br}(\mu\to e\nu\bar{\nu})$	0.99995	0.99997	0.00010	0.229	SM
$\mathrm{Br}(\mu^-\to e^-e^+e^-)\times 10^{13}$	0.000	0	7.8	0.000	[1]
$\mathrm{Br}(\mu\to e\gamma)\times 10^{13}$	2.100	0	3.3	0.641	[1]
$\mathrm{Br}(\tau\to e\nu\bar{\nu})$	0.178510	0.178510	0.000018	0.000	SM
$\mathrm{Br}(\tau\to \mu\nu\bar{\nu})$	0.173608	0.173612	0.000017	0.229	SM
$\mathrm{Br}(\tau^-\to e^-e^+e^-)\times 10^8$	0.000	0	2.1	0.000	[1]
$\mathrm{Br}(\tau^-\to e^-\mu^+e^-)\times 10^8$	0.000	0	1.2	0.000	[1]
$\mathrm{Br}(\tau^-\to \mu^-e^+\mu^-)\times 10^8$	0.000	0	1.3	0.000	[1]
$\mathrm{Br}(\tau^-\to \mu^-\mu^+\mu^-)\times 10^8$	7.4×10^{-3}	0	1.6	0.005	[1]
$\mathrm{Br}(\tau^-\to e^-\mu^+\mu^-)\times 10^8$	0.000	0	2.1	0.000	[1]
$\mathrm{Br}(\tau^-\to \mu^-e^+e^-)\times 10^8$	0.000	0	1.4	0.000	[1]
$\mathrm{Br}(\tau\to e\gamma)\times 10^8$	0.000	0	2.6	0.000	[1]
$\mathrm{Br}(\tau\to \mu\gamma)\times 10^8$	4.9×10^{-2}	0	3.4	0.014	[1]
$\Delta a_e\times 10^{13}$	0.000	−8.700	3.6	2.417	[86]
$\Delta a_\mu\times 10^9$	2.43	2.68	0.76	0.332	[1]

TABLE XII. Observables for SM bosons at point B.

Name	Value	Data	Uncertainty	Pull	Ref.
$\mathrm{Br}(W^+\to e^+\nu)$	0.10862	0.10862	0.00011	0.000	SM
$\mathrm{Br}(W^+\to \mu^+\nu)$	0.10862	0.10862	0.00011	0.023	SM
$\mathrm{Br}(W^+\to \tau^+\nu)$	0.10855	0.10855	0.00011	0.000	SM
$\mathrm{Br}(W\to \mathrm{had})$	0.652	0.666	0.025	0.550	SM
$\mathrm{Br}(W^+\to c\bar{s})$	0.309	0.324	0.032	0.464	SM

(Table continued)

TABLE XII. *(Continued)*

Name	Value	Data	Uncertainty	Pull	Ref.
$\mathrm{Br}(Z \to e^+e^-) \times 10^2$	3.333	3.333	0.0062	0.000	SM
$\mathrm{Br}(Z \to \mu^+\mu^-) \times 10^2$	3.333	3.333	0.0062	0.000	SM
$\mathrm{Br}(Z \to \tau^+\tau^-) \times 10^2$	3.326	3.326	0.0062	0.000	SM
$\mathrm{Br}(Z \to \mathrm{had})$	0.676	0.677	0.025	0.014	SM
$\mathrm{Br}(Z \to u\bar{u} + c\bar{c})/2$	0.1157	0.1157	0.0043	0.000	SM
$\mathrm{Br}(Z \to d\bar{d} + s\bar{s} + b\bar{b})/3$	0.1483	0.1483	0.0056	0.000	SM
$\mathrm{Br}(Z \to c\bar{c})$	0.1157	0.1157	0.0043	0.000	SM
$\mathrm{Br}(Z \to b\bar{b})$	0.1479	0.1479	0.0056	0.000	SM
$\mathrm{Br}(Z \to e\mu) \times 10^7$	0.000	0	4.6	0.000	[1]
$\mathrm{Br}(Z \to e\tau) \times 10^6$	0.000	0	6.0	0.000	[1]
$\mathrm{Br}(Z \to \mu\tau) \times 10^6$	0.000	0	7.3	0.000	[1]
A_e	0.1468	0.1468	0.0015	0.000	SM
A_μ	0.147	0.147	0.015	0.000	SM
A_τ	0.1468	0.1468	0.0015	0.000	SM
A_s	0.941	0.941	0.094	0.000	SM
A_c	0.6949	0.6949	0.0069	0.000	SM
A_b	0.9406	0.9406	0.0094	0.000	SM
$\mu_{\mu\mu}$	0.977	0	1.3	0.752	[1]
$\mu_{\tau\tau}$	0.981	1.12	0.23	0.606	[1]
μ_{bb}	0.843	0.950	0.22	0.488	[1]
$\mu_{\gamma\gamma}$	1.00	1.16	0.18	0.863	[1]
$\mathrm{Br}(h \to e^+e^-) \times 10^3$	4.8×10^{-6}	0	1.2	0.000	[1]
$\mathrm{Br}(h \to e\mu) \times 10^4$	0.000	0	2.1	0.000	[1]
$\mathrm{Br}(h \to e\tau) \times 10^3$	0.000	0	4.2	0.000	[1]
$\mathrm{Br}(h \to \mu\tau) \times 10^3$	0.000	0	8.7	0.000	[1]

TABLE XIII. Quark masses and CKM matrix at the point B.

Name	Value	Data	Uncertainty	Pull	Ref.
$m_u(m_Z)$ (GeV) $\times 10^3$	1.28	1.29	0.39	0.031	[112]
$m_c(m_Z)$ (GeV)	0.629	0.627	0.019	0.096	[112]
$m_t(m_Z)$ (GeV)	171.52	171.68	1.5	0.112	[112]
$m_d(m_Z)$ (GeV) $\times 10^3$	2.74	2.75	0.29	0.032	[112]
$m_s(m_Z)$ (GeV) $\times 10^3$	54.33	54.32	2.9	0.002	[112]
$m_b(m_Z)$ (GeV)	2.85	2.85	0.026	0.052	[112]
$\lvert V_{ud}\rvert$	0.97446	0.97420	0.00021	1.236	[1]
$\lvert V_{us}\rvert$	0.22453	0.22430	0.00050	0.467	[1]
$\lvert V_{ub}\rvert \times 10^3$	3.63	3.94	0.36	0.859	[1]
$\lvert V_{cd}\rvert$	0.2244	0.2180	0.0040	1.598	[1]
$\lvert V_{cs}\rvert$	0.974	0.997	0.017	1.375	[1]
$\lvert V_{cb}\rvert \times 10^2$	4.14	4.22	0.080	1.010	[1]
$\lvert V_{td}\rvert \times 10^3$	8.72	8.10	0.50	1.233	[1]
$\lvert V_{ts}\rvert \times 10^2$	4.06	3.94	0.23	0.533	[1]
$\lvert V_{tb}\rvert$	0.999	1.02	0.025	0.795	[1]
α	1.54	1.47	0.097	0.640	[1]
$\sin 2\beta$	0.704	0.691	0.017	0.768	[1]
γ	1.21	1.28	0.081	0.845	[1]

TABLE XIV. Observables for quarks at point B.

Name	Value	Data	Uncertainty	Pull	Ref.
ΔM_K (ps^{-1}) $\times 10^3$	6.015	5.293	2.2	0.333	[1]
$\epsilon_K \times 10^3$	2.21	2.23	0.21	0.081	[1]
ΔM_{B_d} (ps^{-1})	0.599	0.506	0.081	1.139	[1]
$S_{\psi K_s}$	0.686	0.695	0.019	0.475	[85]
ΔM_{B_s} (ps^{-1})	19.81	17.76	2.5	0.826	[1]
$S_{\psi\phi} \times 10^2$	3.627	2.100	3.1	0.493	[85]
$\lvert x_{12}^D\rvert \times 10^3$	2.0×10^{-2}	0	5.0	0.004	SM
$R_K^{\nu\nu}$	1.133	1.000	3.4	0.040	[113]
$R_{K^*}^{\nu\nu}$	1.133	1.000	3.4	0.039	[114]
$R_{B_d\to\mu\mu}$	0.877	1.509	1.4	0.445	[1,115,116]
$R_{B_s\to\mu\mu}$	0.864	0.750	0.16	0.722	[1,115,116]
Γ_t	1.49	1.41	0.17	0.485	[1]
$\mathrm{Br}(t\to Zq) \times 10^4$	0.000	0	3.0	0.000	[1]
$\mathrm{Br}(t\to Zu) \times 10^3$	0.000	0	1.5	0.000	[1]
$\mathrm{Br}(t\to Zc) \times 10^3$	0.000	0	1.3	0.000	[1]
$\mathrm{Re}C_9^\mu$	−0.571	−0.700	0.30	0.431	[30]
$\mathrm{Im}C_9^\mu$	-1.0×10^{-2}	0	0.10	0.103	[30]
$\mathrm{Re}C_{10}^\mu$	0.316	0.400	0.20	0.421	[30]
$\mathrm{Im}C_{10}^\mu$	5.7×10^{-3}	0	0.10	0.057	[30]
$\mathrm{Re}C_9^{\prime\mu}$	-2.5×10^{-4}	0	0.10	0.002	[30]
$\mathrm{Im}C_9^{\prime\mu}$	1.9×10^{-4}	0	0.10	0.002	[30]
$\mathrm{Re}C_{10}^{\prime\mu}$	1.4×10^{-4}	0	0.10	0.001	[30]
$\mathrm{Im}C_{10}^{\prime\mu}$	-1.1×10^{-4}	0	0.10	0.001	[30]
$\mathrm{Br}(B\to K\tau^+\tau^-) \times 10^3$	1.2×10^{-4}	0	1.8	0.000	[117]

[1] M. Tanabashi *et al.* (Particle Data Group), Review of particle physics, Phys. Rev. D **98**, 030001 (2018).

[2] G. W. Bennett *et al.* (Muon g-2 Collaboration), Final report of the Muon E821 anomalous magnetic moment measurement at BNL, Phys. Rev. D **73**, 072003 (2006).

[3] R. Aaij *et al.* (LHCb Collaboration), Test of Lepton Universality Using $B^+ \to K^+\ell^+\ell^-$ Decays, Phys. Rev. Lett. **113**, 151601 (2014).

[4] R. Aaij *et al.* (LHCb Collaboration), Test of lepton universality with $B^0 \to K^{*0}\ell^+\ell^-$ decays, J. High Energy Phys. 08 (2017) 055.

[5] R. Aaij *et al.* (LHCb Collaboration), Search for Lepton-Universality Violation in $B^+ \to K^+\ell^+\ell^-$ Decays, Phys. Rev. Lett. **122**, 191801 (2019).

[6] A. Abdesselam *et al.* (Belle Collaboration), Test of lepton flavor universality in $B \to K^*\ell^+\ell^-$ decays at Belle, arXiv: 1904.02440.

[7] R. Aaij *et al.* (LHCb Collaboration), Differential branching fraction and angular analysis of the decay $B_s^0 \to \phi\mu^+\mu^-$, J. High Energy Phys. 07 (2013) 084.

[8] J. P. Lees *et al.* (*BABAR* Collaboration), Measurement of the $B \to X_s l^+ l^-$ Branching Fraction and Search for Direct *CP* Violation from a Sum of Exclusive Final States, Phys. Rev. Lett. **112**, 211802 (2014).

[9] R. Aaij *et al.* (LHCb Collaboration), Differential branching fractions and isospin asymmetries of $B \to K^{(*)}\mu^+\mu^-$ decays, J. High Energy Phys. 06 (2014) 133.

[10] R. Aaij *et al.* (LHCb Collaboration), Angular analysis and differential branching fraction of the decay $B_s^0 \to \phi\mu^+\mu^-$, J. High Energy Phys. 09 (2015) 179.

[11] R. Aaij *et al.* (LHCb Collaboration), Measurement of Form-Factor-Independent Observables in the Decay $B^0 \to K^{*0}\mu^+\mu^-$, Phys. Rev. Lett. **111**, 191801 (2013).

[12] V. Khachatryan *et al.* (CMS Collaboration), Angular analysis of the decay $B^0 \to K^{*0}\mu^+\mu^-$ from pp collisions at $\sqrt{s} = 8$ TeV, Phys. Lett. B **753**, 424 (2016).

[13] R. Aaij *et al.* (LHCb Collaboration), Angular analysis of the $B^0 \to K^{*0}\mu^+\mu^-$ decay using 3 fb^{-1} of integrated luminosity, J. High Energy Phys. 02 (2016) 104.

[14] A. Abdesselam *et al.* (Belle Collaboration), Angular analysis of $B^0 \to K^*(892)^0\ell^+\ell^-$, in *Proceedings, LHCSki*

2016—A First Discussion of 13 TeV Results: Obergurgl, Austria (2016).
[15] S. Wehle *et al.* (Belle Collaboration), Lepton-Flavor-Dependent Angular Analysis of $B \to K^* \ell^+ \ell^-$, Phys. Rev. Lett. **118**, 111801 (2017).
[16] ATLAS Collaboration, Angular analysis of $B_d^0 \to K^* \mu^+ \mu^-$ decays in pp collisions at $\sqrt{s} = 8$ TeV with the ATLAS detector, J. High Energy Phys. 10 (2018) 047.
[17] CMS Collaboration, Measurement of the P_1 and P_5' angular parameters of the decay $\mathrm{B}^0 \to \mathrm{K}^{*0} \mu^+ \mu^-$ in proton-proton collisions at $\sqrt{s} = 8$ TeV.
[18] A. J. Buras and M. Munz, Effective Hamiltonian for $B \to X(s) e^+ e^-$ beyond leading logarithms in the NDR and HV schemes, Phys. Rev. D **52**, 186 (1995).
[19] C. Bobeth, M. Misiak, and J. Urban, Photonic penguins at two loops and m_t dependence of $\mathrm{BR}[B \to X_s l^+ l^-]$, Nucl. Phys. **B574**, 291 (2000).
[20] B. Grinstein, M. J. Savage, and M. B. Wise, $B \to X(s) e^+ e^-$ in the six quark model, Nucl. Phys. **B319**, 271 (1989).
[21] W. Altmannshofer, C. Niehoff, P. Stangl, and D. M. Straub, Status of the $B \to K^* \mu^+ \mu^-$ anomaly after Moriond 2017, Eur. Phys. J. C **77**, 377 (2017).
[22] W. Altmannshofer, P. Stangl, and D. M. Straub, Interpreting hints for Lepton flavor universality violation, Phys. Rev. D **96**, 055008 (2017).
[23] A. K. Alok, B. Bhattacharya, A. Datta, D. Kumar, J. Kumar, and D. London, New physics in $b \to s \mu^+ \mu^-$ after the measurement of R_{K^*}, Phys. Rev. D **96**, 095009 (2017).
[24] B. Capdevila, A. Crivellin, S. Descotes-Genon, J. Matias, and J. Virto, Patterns of new physics in $b \to s \ell^+ \ell^-$ transitions in the light of recent data, J. High Energy Phys. 01 (2018) 093.
[25] M. Ciuchini, A. M. Coutinho, M. Fedele, E. Franco, A. Paul, L. Silvestrini, and M. Valli, On flavourful easter eggs for new physics hunger and lepton flavour universality violation, Eur. Phys. J. C **77**, 688 (2017).
[26] G. D'Amico, M. Nardecchia, P. Panci, F. Sannino, A. Strumia, R. Torre, and A. Urbano, Flavour anomalies after the R_{K^*} measurement, J. High Energy Phys. 09 (2017) 010.
[27] L.-S. Geng, B. Grinstein, S. Jäger, J. M. Camalich, X.-L. Ren, and R.-X. Shi, Towards the discovery of new physics with lepton-universality ratios of $b \to s \ell \ell$ decays, Phys. Rev. D **96**, 093006 (2017).
[28] D. Ghosh, Explaining the R_K and R_{K^*} anomalies, Eur. Phys. J. C **77**, 694 (2017).
[29] A. Arbey, T. Hurth, F. Mahmoudi, and S. Neshatpour, Hadronic and new physics contributions to $b \to s$ transitions, Phys. Rev. D **98**, 095027 (2018).
[30] J. Aebischer, W. Altmannshofer, D. Guadagnoli, M. Reboud, P. Stangl, and D. M. Straub, B-decay discrepancies after Moriond 2019, arXiv:1903.10434.
[31] M. Algueró, B. Capdevila, A. Crivellin, S. Descotes-Genon, P. Masjuan, J. Matias, and J. Virto, Addendum: "Patterns of New Physics in $b \to s \ell^+ \ell^-$ transitions in the light of recent data" and "Are we overlooking Lepton Flavour Universal New Physics in $b \to s \ell \ell$?", Eur. Phys. J. C **79**, 714 (2019).
[32] A. K. Alok, A. Dighe, S. Gangal, and D. Kumar, Continuing search for new physics in $b \to s \mu \mu$ decays: Two operators at a time, J. High Energy Phys. 06 (2019) 089.
[33] M. Ciuchini, A. M. Coutinho, M. Fedele, E. Franco, A. Paul, L. Silvestrini, and M. Valli, New physics in $b \to s \ell^+ \ell^-$ confronts new data on lepton universality, arXiv:1903.09632.
[34] A. Datta, J. Kumar, and D. London, The B anomalies and new physics in $b \to s e^+ e^-$, arXiv:1903.10086.
[35] K. Kowalska, D. Kumar, and E. M. Sessolo, Implications for new physics in $b \to s \mu \mu$ transitions after recent measurements by Belle and LHCb, arXiv:1903.10932.
[36] A. Arbey, T. Hurth, F. Mahmoudi, D. M. Santos, and S. Neshatpour, Update on the b → s anomalies, Phys. Rev. D **100**, 015045 (2019).
[37] D. Kumar, K. Kowalska, and E. M. Sessolo, Global Bayesian Analysis of New Physics in b→sμμ Transitions after Moriond-2019, in *17th Conference on Flavor Physics and CP Violation (FPCP 2019) Victoria, BC, Canada* (2019).
[38] A. Czarnecki and W. J. Marciano, The Muon anomalous magnetic moment: A Harbinger for 'new physics', Phys. Rev. D **64**, 013014 (2001).
[39] K. Kannike, M. Raidal, D. M. Straub, and A. Strumia, Anthropic solution to the magnetic muon anomaly: The charged see-saw, J. High Energy Phys. 02 (2012) 106; Erratum, J. High Energy Phys. 10 (2012) 136(E).
[40] R. Dermisek and A. Raval, Explanation of the Muon g-2 anomaly with vectorlike leptons and its implications for Higgs decays, Phys. Rev. D **88**, 013017 (2013).
[41] M. Lindner, M. Platscher, and F. S. Queiroz, A call for new physics: The Muon anomalous magnetic moment and lepton flavor violation, Phys. Rep. **731**, 1 (2018).
[42] W. Altmannshofer, S. Gori, M. Pospelov, and I. Yavin, Quark flavor transitions in $L_\mu - L_\tau$ models, Phys. Rev. D **89**, 095033 (2014).
[43] A. Crivellin, G. D'Ambrosio, and J. Heeck, Explaining $h \to \mu^\pm \tau^\mp$, $B \to K^* \mu^+ \mu^-$ and $B \to K \mu^+ \mu^- / B \to K e^+ e^-$ in a two-Higgs-Doublet Model with Gauged $L_\mu - L_\tau$, Phys. Rev. Lett. **114**, 151801 (2015).
[44] S. F. King, Flavourful Z' models for $R_{K^{(*)}}$, J. High Energy Phys. 08 (2017) 019.
[45] B. Allanach, F. S. Queiroz, A. Strumia, and S. Sun, Z' models for the LHCb and $g-2$ muon anomalies, Phys. Rev. D **93**, 055045 (2016); Erratum, Phys. Rev. D **95**, 119902(E) (2017).
[46] W. Altmannshofer, M. Carena, and A. Crivellin, $L_\mu - L_\tau$ theory of Higgs flavor violation and $(g-2)_\mu$, Phys. Rev. D **94**, 095026 (2016).
[47] E. Megias, M. Quiros, and L. Salas, $g_\mu - 2$ from vector-like leptons in warped space, J. High Energy Phys. 05 (2017) 016.
[48] S. Raby and A. Trautner, Vectorlike chiral fourth family to explain muon anomalies, Phys. Rev. D **97**, 095006 (2018).
[49] L. Darmé, K. Kowalska, L. Roszkowski, and E. M. Sessolo, Flavor anomalies and dark matter in SUSY with an extra U(1), J. High Energy Phys. 10 (2018) 052.
[50] B. Gripaios, M. Nardecchia, and S. A. Renner, Linear flavour violation and anomalies in B physics, J. High Energy Phys. 06 (2016) 083.

[51] P. Arnan, L. Hofer, F. Mescia, and A. Crivellin, Loop effects of heavy new scalars and fermions in $b \to s\mu^+\mu^-$, J. High Energy Phys. 04 (2017) 043.

[52] B. Grinstein, S. Pokorski, and G. G. Ross, Lepton non-universality in B decays and fermion mass structure, J. High Energy Phys. 12 (2018) 079.

[53] P. Arnan, A. Crivellin, M. Fedele, and F. Mescia, Generic loop effects of new scalars and Fermions in $b \to s\ell^+\ell^-$ and a vector-like 4th generation, J. High Energy Phys. 06 (2019) 118.

[54] C.-W. Chiang and H. Okada, A simple model for explaining muon-related anomalies and dark matter, Int. J. Mod. Phys. A **34**, 1950106 (2019).

[55] J. M. Cline and J. M. Cornell, $R(K^{(*)})$ from dark matter exchange, Phys. Lett. B **782**, 232 (2018).

[56] J. Kawamura, S. Okawa, and Y. Omura, Interplay between the $b \to s\ell\ell$ anomalies and dark matter physics, Phys. Rev. D **96**, 075041 (2017).

[57] B. Barman, D. Borah, L. Mukherjee, and S. Nandi, Correlating the anomalous results in $b \to s$ decays with inert Higgs doublet dark matter and muon $(g-2)$, arXiv:1808.06639.

[58] D. G. Cerdeño, A. Cheek, P. Martín-Ramiro, and J. M. Moreno, B anomalies and dark matter: a complex connection, Eur. Phys. J. C **79**, 517 (2019).

[59] D. A. Sierra, F. Staub, and A. Vicente, Shedding light on the $b \to s$ anomalies with a dark sector, Phys. Rev. D **92**, 015001 (2015).

[60] A. Falkowski, S. F. King, E. Perdomo, and M. Pierre, Flavourful Z' portal for vector-like neutrino Dark Matter and $R_{K^{(*)}}$, J. High Energy Phys. 08 (2018) 061.

[61] V. Bernard, M. Oertel, E. Passemar, and J. Stern, Tests of non-standard electroweak couplings of right-handed quarks, J. High Energy Phys. 01 (2008) 015.

[62] F. Jegerlehner and A. Nyffeler, The Muon g-2, Phys. Rep. **477**, 1 (2009).

[63] L. Lavoura, General formulae for $f(1) \to f(2)\gamma$, Eur. Phys. J. C **29**, 191 (2003).

[64] A. J. Buras, F. De Fazio, and J. Girrbach, The anatomy of Z' and Z with flavour changing neutral currents in the flavour precision era, J. High Energy Phys. 02 (2013) 116.

[65] L. Di Luzio, M. Kirk, and A. Lenz, Updated B_s-mixing constraints on new physics models for $b \to s\ell^+\ell^-$ anomalies, Phys. Rev. D **97**, 095035 (2018).

[66] A. J. Buras and J. Girrbach, Complete NLO QCD corrections for tree level delta $F = 2$ FCNC processes, J. High Energy Phys. 03 (2012) 052.

[67] T. Inami and C. S. Lim, Effects of superheavy quarks and leptons in low-energy weak processes k(L) → mu anti-mu, K+ → pi + neutrino anti-neutrino and K0 ↔ anti-K0, Prog. Theor. Phys. **65**, 297 (1981); Erratum, Prog. Theor. Phys. **65**, 1772(E) (1981).

[68] A. J. Buras, M. Jamin, and P. H. Weisz, Leading and next-to-leading QCD corrections to ϵ parameter and $B^0 - \bar{B}^0$ mixing in the presence of a heavy top quark, Nucl. Phys. **B347**, 491 (1990).

[69] J. Urban, F. Krauss, U. Jentschura, and G. Soff, Next-to-leading order QCD corrections for the B0 anti-B0 mixing with an extended Higgs sector, Nucl. Phys. **B523**, 40 (1998).

[70] S. Aoki *et al.* (Flavour Lattice Averaging Group), FLAG review 2019, arXiv:1902.08191.

[71] N. Carrasco *et al.* (ETM Collaboration), B-physics from $N_f = 2$ tmQCD: The Standard Model and beyond, J. High Energy Phys. 03 (2014) 016.

[72] A. Bazavov *et al.* (Fermilab Lattice and MILC Collaborations), $B^0_{(s)}$-mixing matrix elements from lattice QCD for the Standard Model and beyond, Phys. Rev. D **93**, 113016 (2016).

[73] N. Carrasco *et al.*, $D^0 - \bar{D}^0$ mixing in the Standard Model and beyond from $N_f = 2$ twisted mass QCD, Phys. Rev. D **90**, 014502 (2014).

[74] A. J. Buras, S. Jager, and J. Urban, Master formulae for Delta $F = 2$ NLO QCD factors in the Standard Model and beyond, Nucl. Phys. **B605**, 600 (2001).

[75] D. King, A. Lenz, and T. Rauh, B_s mixing observables and —V_{td}/V_{ts}—from sum rules, J. High Energy Phys. 05 (2019) 034.

[76] D. Geiregat *et al.* (CHARM-II Collaboration), First observation of neutrino trident production, Phys. Lett. B **245**, 271 (1990).

[77] S. R. Mishra *et al.* (CCFR Collaboration), Neutrino Tridents and W Z Interference, Phys. Rev. Lett. **66**, 3117 (1991).

[78] T. Adams *et al.* (NuTeV Collaboration), Evidence for diffractive charm production in muon-neutrino Fe and anti-muon-neutrino Fe scattering at the Tevatron, Phys. Rev. D **61**, 092001 (2000).

[79] W. Altmannshofer, S. Gori, M. Pospelov, and I. Yavin, Neutrino Trident Production: A Powerful Probe of New Physics with Neutrino Beams, Phys. Rev. Lett. **113**, 091801 (2014).

[80] G. Magill and R. Plestid, Neutrino trident production at the intensity frontier, Phys. Rev. D **95**, 073004 (2017).

[81] S.-F. Ge, M. Lindner, and W. Rodejohann, Atmospheric trident production for probing new physics, Phys. Lett. B **772**, 164 (2017).

[82] P. Ballett, M. Hostert, S. Pascoli, Y. F. Perez-Gonzalez, Z. Tabrizi, and R. Z. Funchal, Neutrino trident scattering at near detectors, J. High Energy Phys. 01 (2019) 119.

[83] W. Altmannshofer, S. Gori, J. Martín-Albo, A. Sousa, and M. Wallbank, Neutrino tridents at DUNE, arXiv:1902.06765.

[84] A. Hook, E. Izaguirre, and J. G. Wacker, Model independent bounds on kinetic mixing, Adv. High Energy Phys. **2011**, 859762 (2011).

[85] Y. Amhis *et al.* (HFLAV Collaboration), Averages of b-hadron, c-hadron, and τ-lepton properties as of summer 2016, Eur. Phys. J. C **77**, 895 (2017).

[86] H. Davoudiasl and W. J. Marciano, Tale of two anomalies, Phys. Rev. D **98**, 075011 (2018).

[87] A. Crivellin, M. Hoferichter, and P. Schmidt-Wellenburg, Combined explanations of $(g-2)_{\mu,e}$ and implications for a large muon EDM, Phys. Rev. D **98**, 113002 (2018).

[88] J. Liu, C. E. M. Wagner, and X.-P. Wang, A light complex scalar for the electron and muon anomalous magnetic moments, J. High Energy Phys. 03 (2019) 008.

[89] B. Dutta and Y. Mimura, Electron $g-2$ with flavor violation in MSSM, Phys. Lett. B **790**, 563 (2019).

[90] R. H. Parker, C. Yu, W. Zhong, B. Estey, and H. Müller, Measurement of the fine-structure constant as a test of the Standard Model, Science **360**, 191 (2018).

[91] X.-F. Han, T. Li, L. Wang, and Y. Zhang, Simple interpretations of lepton anomalies in the lepton-specific inert two-Higgs-doublet model, Phys. Rev. D **99**, 095034 (2019).

[92] M. Endo and W. Yin, Explaining electron and muon $g-2$ anomaly in SUSY without lepton-flavor mixings, J. High Energy Phys. 08 (2019) 122.

[93] M. Kohda, T. Modak, and A. Soffer, Identifying a Z' behind $b \to s\ell\ell$ anomalies at the LHC, Phys. Rev. D **97**, 115019 (2018).

[94] B. C. Allanach, J. M. Butterworth, and T. Corbett, Collider constraints on Z' models for neutral current B-anomalies, arXiv:1904.10954.

[95] G. Aad *et al.* (ATLAS Collaboration), Search for high-mass dilepton resonances using 139 fb^{-1} of pp collision data collected at $\sqrt{s} = 13$ TeV with the ATLAS detector, Phys. Lett. B **796**, 68 (2019).

[96] J. Alwall, R. Frederix, S. Frixione, V. Hirschi, F. Maltoni, O. Mattelaer, H. S. Shao, T. Stelzer, P. Torrielli, and M. Zaro, The automated computation of tree-level and next-to-leading order differential cross sections, and their matching to parton shower simulations, J. High Energy Phys. 07 (2014) 079.

[97] C. Degrande, C. Duhr, B. Fuks, D. Grellscheid, O. Mattelaer, and T. Reiter, UFO–The Universal FeynRules output, Comput. Phys. Commun. **183**, 1201 (2012).

[98] N. D. Christensen and C. Duhr, FeynRules–Feynman rules made easy, Comput. Phys. Commun. **180**, 1614 (2009).

[99] Z. Poh and S. Raby, Vectorlike leptons: Muon g-2 anomaly, lepton flavor violation, Higgs boson decays, and lepton nonuniversality, Phys. Rev. D **96**, 015032 (2017).

[100] Y. Aoki, T. Ishikawa, T. Izubuchi, C. Lehner, and A. Soni, Neutral B meson mixings and B meson decay constants with static heavy and domain-wall light quarks, Phys. Rev. D **91**, 114505 (2015).

[101] E. Gamiz, C. T. H. Davies, G. P. Lepage, J. Shigemitsu, and M. Wingate (HPQCD Collaboration), Neutral B meson mixing in unquenched lattice QCD, Phys. Rev. D **80**, 014503 (2009).

[102] B. Belfatto, R. Beradze, and Z. Berezhiani, The CKM unitarity problem: A trace of new physics at the TeV scale?, arXiv:1906.02714.

[103] G. Aad *et al.* (ATLAS Collaboration), Search for heavy lepton resonances decaying to a Z boson and a lepton in pp collisions at $\sqrt{s} = 8$ TeV with the ATLAS detector, J. High Energy Phys. 09 (2015) 108.

[104] R. Dermisek, J. P. Hall, E. Lunghi, and S. Shin, Limits on vectorlike leptons from searches for anomalous production of multi-lepton events, J. High Energy Phys. 12 (2014) 013.

[105] A. M. Sirunyan *et al.* (CMS Collaboration), Search for vector-like leptons in multilepton final states in proton-proton collisions at $\sqrt{s} = 13$ TeV, arXiv:1905.10853.

[106] P. N. Bhattiprolu and S. P. Martin, Prospects for vectorlike leptons at future proton-proton colliders, Phys. Rev. D **100**, 015033 (2019).

[107] N. Kumar and S. P. Martin, Vectorlike leptons at the large hadron collider, Phys. Rev. D **92**, 115018 (2015).

[108] A. Falkowski, D. M. Straub, and A. Vicente, Vector-like leptons: Higgs decays and collider phenomenology, J. High Energy Phys. 05 (2014) 092.

[109] S. A. R. Ellis, R. M. Godbole, S. Gopalakrishna, and J. D. Wells, Survey of vector-like fermion extensions of the Standard Model and their phenomenological implications, J. High Energy Phys. 09 (2014) 130.

[110] M. Aaboud *et al.* (ATLAS Collaboration), Search for pair production of heavy vector-like quarks decaying to high-p_T W bosons and b quarks in the lepton-plus-jets final state in pp collisions at $\sqrt{s} = 13$ TeV with the ATLAS detector, J. High Energy Phys. 10 (2017) 141.

[111] M. Aaboud *et al.* (ATLAS Collaboration), Search for pair production of up-type vector-like quarks and for four-top-quark events in final states with multiple b-jets with the ATLAS detector, J. High Energy Phys. 07 (2018) 089.

[112] S. Antusch and V. Maurer, Running quark and lepton parameters at various scales, J. High Energy Phys. 11 (2013) 115.

[113] J. P. Lees *et al.* (*BABAR* Collaboration), Search for $B \to K^{(*)}\nu\bar{\nu}$ and invisible quarkonium decays, Phys. Rev. D **87**, 112005 (2013).

[114] O. Lutz *et al.* (Belle Collaboration), Search for $B \to h^{(*)}\nu\bar{\nu}$ with the full Belle $\Upsilon(4S)$ data sample, Phys. Rev. D **87**, 111103 (2013).

[115] W. Altmannshofer, C. Niehoff, and D. M. Straub, $B_s \to \mu^+\mu^-$ as current and future probe of new physics, J. High Energy Phys. 05 (2017) 076.

[116] C. Bobeth, M. Gorbahn, T. Hermann, M. Misiak, E. Stamou, and M. Steinhauser, $B_{s,d} \to l^+l^-$ in the Standard Model with Reduced Theoretical Uncertainty, Phys. Rev. Lett. **112**, 101801 (2014).

[117] J. P. Lees *et al.* (*BABAR* Collaboration), Search for $B^+ \to K^+\tau^+\tau^-$ at the *BABAR* Experiment, Phys. Rev. Lett. **118**, 031802 (2017).